Development of Cathodic Electrocatalysts for Use in Low Temperature H_2/O_2 Fuel Cells with an Alkaline Electrolyte

Contract No. NASW-1233

Q-7

Seventh Quarterly Report
Covering January 1, 1967
Through March 31, 1967

for

National Aeronautics and Space Administration
Headquarters, Washington, D. C.

NOTICE

DEVELOPMENT OF CATHODIC ELECTROCATALYSTS FOR USE IN LOW TEMPERATURE H_2/O_2 FUEL CELLS WITH AN ALKALINE ELECTROLYTE

Contract No. NASW-1233

Q-7

Seventh Quarterly Report
Covering January 1, 1967
Through March 31, 1967

by

J. Giner
J. Parry
L. Swette
R. Cattabriga

for
National Aeronautics and Space
Administration
Headquarters, Washington, D. C.

CONTRACT OBJECTIVES

The research under contract NASW-1233 is directed towards the development of an improved oxygen electrode for use in alkaline H_2/O_2 fuel cells. The work is being carried out for the National Aeronautics and Space Administration, with Mr. E. Cohn as technical monitor. Principal investigators are Dr. J. Giner, and Dr. J. Parry.

CONTENTS

CONTENTS (Cont' d)

ABSTRACT

Carbides and nitrocarbides of nickel, cobalt and nickel/cobalt alloys prepared by the Bureau of Mines by direct carbiding and nitriding of the Raney metals were tested for activity in the reduction of O_2 in basic electrolyte. Nickel carbide was also prepared at Tyco by decomposition of nickel acetate. These catalysts were tested in practical electrode structures – PTFE bonded screen electrodes; it was apparent that the catalysts derived from the Raney metals do not have the proper physical form to produce high performance electrodes. This was established by comparing the two types of Ni_3C catalysts. Electrodes made with Ni_3C obtained by acetate decomposition showed an activity in the best case of 100 ma/cm^2 at 750 mv and a limiting current of > 250 ma/cm^2. However, the highest performance measured for the Raney catalyst was 37 ma/cm^2 at 750 mv and a limiting current of < 100 ma/cm^2. Furthermore, by comparing the activity of the Raney metals and the interstitial compounds prepared from them it can be seen that the performance is lowered by carbiding and nitriding, probably because of sintering during the carbiding process.

With the exception of the nitrocarbides, the activity of the nickel/cobalt alloys is in the order 3 Ni/Co > Ni/Co > Ni/3 Co. For example, with the carbides of these alloys the current densities at 750 mv were 24 ma/cm^2, 16 ma/cm^2, and 12 ma/cm^2, respectively. It should be stressed here that the actual current densities recorded do not truly reflect the intrinsic activity of these catalysts, which are potentially capable of supporting much higher current densities. The performances quoted are low as a result of improper pore structure of the catalyst itself which results in an inefficient electrode structure. During the testing of these catalysts it was noted that the activity initially increased to a steady value (in less than 1 hour) and then decayed to a constant value (over a few hours) at about half the initial performance. Experimental techniques were established to ensure that the plateau, or first steady value, was recorded. This is justified on the basis that this performance can be stabilized.

A 30% Au-70% Pd black was tested as a PTFE bonded electrode. At 950 mv this electrode produced 60 ma/cm^2 compared with 32 ma/cm^2 for a Pt black electrode prepared in a similar manner.

A detailed study of nonstoichiometric TiO_2, including single crystalline rutile, was begun. A better understanding of the catalytic behavior of this material towards O_2 reduction is required if there is to be a possibility of exploiting Ti_3Au as a practical catalyst. Four more intermetallic compounds were tested which are related to Ti_3Au ($E_{1/2}$ = 810 mv). These were V_3Au (corrodes rapidly), and Nb_3Au ($E_{1/2}$ = 825 mv, with corrosion), $TiAu_2$ ($E_{1/2}$ = 725 mv), and TiAu ($E_{1/2}$ = 745 mv). Finally, two materials were retested using improved techniques and lower operating temperature. These are $TiRh_3$ ($E_{1/2}$ = 610 mv) and $TiAu_{1.5}Rh_{1.5}$ ($E_{1/2}$ = 825 mv). The half wave potentials were significantly higher than found previously.

PART 1

THE TESTING OF INTERSTITIAL COMPOUNDS OF NICKEL AND COBALT

I. INTRODUCTION

This part of the study is concerned with the investigation of the catalytic activity of carbides and nitrocarbides of nickel, cobalt and nickel/cobalt alloys towards the cathodic reduction of O_2. It represents a more detailed examination of these types of materials, prepared mainly by the Bureau of Mines, Pittsburgh Coal Research Center, following some earlier encouraging results obtained with Ni_3C and nickel/cobalt carbide prepared in our laboratory.

Further samples of laboratory-made catalysts were also prepared and tested because the preparative method was known to give a catalyst of very different physical character, particularly a lower bulk density*. The catalysts were tested as PTFE bonded electrodes, a structure designed to provide one good mass transport condition required for the electrode process. However, this is achieved only when the catalysts themselves can contribute favorable physical characteristics; without them the electrode polarizes rapidly. Qualitatively, a low bulk density indicates a large amount of void space in the agglomerates of the catalysts. Large parts of these void regions are wet-proofed by the PTFE dispersion and provide good gas transport to all parts of the electrode when the electrode is in contact with the electrolyte.

---

* The Bureau of Mines' catalysts were prepared by direct nitriding or carbiding of Raney metals (see Bureau of Mines' monthly reports), whereas the Tyco materials (carbides) were prepared by thermal decomposition of the acetates.

The smaller pores of the catalyst are too small to be filled with the PTFE dispersion (PTFE particles $\sim 0.1\,\mu$) and become filled with electrolyte by capillary forces. This electrolyte provides the electrical continuity between the active surface of the catalyst within the electrode structure and the bulk of the electrolyte. A catalyst with a large pore volume in the range of pore diameter up to several hundred angstrom units reduces the iR losses in the electrolyte in the electrode structure and promotes efficient use of all the available area of the catalyst.

The electrochemical measurements consisted of current voltage curves obtained under potentiostatic conditions in 35% KOH under O_2 at 75° C. Both manual and slow potential sweep methods were used, and in some cases the corrosion rate was assessed by similar measurements under N_2. The results are presented in the form of tables of current at potentials of 750 mv and 600 mv vs. RHE, so that the activities can be compared easily (Tables I - IV). For a catalyst of good intrinsic activity, the current at 600 mv reflects the capacity of the electrode structure to promote the mass transport processes associated with the reaction. The figure at 750 mv gives an assessment of the intrinsic activity of the catalyst, but this figure is also influenced by electrode structure if the intrinsic activity is high.

II. EXPERIMENTAL

A. Raney Alloy Based Catalysts

These materials were furnished by the Bureau of Mines under an atmosphere of CO_2; the first procedure was to separate each catalyst into eight samples in an nitrogen atmosphere. The catalysts were tested in two forms: the first was obtained by slowly exposing one of the samples to air prior to electrode fabrication; the second, by an induction procedure intended to protect the catalyst from the heat evolved in a rapid oxidation process (such as would take place on immediate exposure to 1 atm O_2). This was carried out as follows: The catalyst was covered with petroleum ether while in an nitrogen atmosphere and then brought out into the air. The liquid layer was then progressively changed (keeping the catalyst covered at all times) through a sequence of solvents in which the solubility of oxygen increases. The solvents were diethyl ether, acetone and methanol. Finally, the methanol was allowed to evaporate exposing the catalyst slowly to air. During this induction process the surface of the catalyst is oxidized slowly. Slow oxidation avoids sintering and may also promote the formation of a coherent oxide film which would reduce the rate of any further oxidation or corrosion process in the electrolyte.

B. Catalysts Formed by Acetate Decomposition

Further samples of nickel carbide and nickel cobalt were prepared by acetate decomposition at Tyco to confirm previous results and to demonstrate that active electrodes could be prepared using a PTFE binder*. Also, as discussed above, differences in the physical structure between catalysts obtained by acetate decomposition and by gas phase carbiding were investigated.

Details of the preparation of Tyco catalysts by thermal decomposition of the acetate salts are given in Table I, page 12.

---

*In the study of interstitial compounds of iron it was found that better performance was obtained from electrodes that were prepared with a binder (ELVAX) not requiring sintering at 275° C[(1)]. However, the oxidation resistance of Elvax is limited.

C. Electrode Preparation

Electrode fabrication consisted of the mixing of the catalyst (after induction or exposure) with a dispersion of PTFE (DuPont, Teflon 30) in a known weight ratio. This mixture was pasted on a nickel screen (100 mesh) to produce an electrode of ~ 6 cm^2 area. The electrodes were dried in a vacuum oven at 100° C and subsequently sintered in a stream of N_2 at 275° C. Several test electrodes of 1 cm^2 area could be cut from the sintered structure. The sintered structures prepared from a particular catalyst are identified, as in Table II, by a number in parentheses, e.g. 26 C (i) and 26 C (ii). Each test electrode is identified by a further letter; e.g. 26 C (i)a and 26 C (i)b are two test electrodes cut from the same sintered structure.

D. Electrochemical Testing

The fabricated electrodes were tested in a floating electrode cell configuration[2] in 35% KOH at 75° C using as reference a dynamic hydrogen electrode[3]. The results are presented in Tables I through IV, pp. 12-16. Current-voltage curves were determined under potentiostatic conditions using the following procedures. For the first measurements on nickel based catalysts, the electrode made contact with the electrolyte at a controlled potential of 1000 mv; the potential was almost immediately reduced to 850 mv and the current noted. The current was measured again after five minutes, the potential was adjusted to 750 mv, and the current measured as before. The current voltage curve was then determined at 50 mv intervals, each held for 5 min in the sequence 750 mv → 400 mv → 850 mv. For the cobalt and nickel-cobalt alloys the procedure was modified to include an anodic induction at 1600 mv for 10 min. The anodic pretreatment induction should produce complete oxidation of the surface and effectively reduce the corrosion rate during oxygen reduction, particularly with the cobalt catalysts. In the case of the nickel-cobalt alloys, the high pretreatment potentials (which may be imagined as being equivalent to heating in an oxidizing atmosphere) could contribute to the formation of a surface spinel ($NiCo_2O_4$), reported[4] to exhibit good conductivity and catalytic activity for oxygen reduction. The complete E (i) curve

850 mv $\rightarrow$ 400 mv $\rightarrow$ 850 mv was measured as before.

Further modifications to the technique were introduced when experiments described in detail in Part 1, section IV, showed that, as previously reported[5], the activity of these electrodes varied with time in an unusual manner. The current at constant potential initially increased, then remained constant for a period of time before decaying to a constant value somewhat below the initial current.

In order to compare the catalytic activity of individual samples, it was obvious that the measurements had to be made at identical points on this time curve. Since this behavior must be related to the surface oxide, two factors probably need to be taken into account: the total time the catalyst was exposed to air before testing (whether inducted or directly exposed) and the total time of exposure to electrolyte during tests.

After the initial examples the first factor was easily eliminated by preparing each electrode individually and testing as soon as possible (usually within 24 hours). Total contact time with the electrolyte was more difficult. If the fabricated electrodes were fully reproducible, complete information could have been obtained by measuring first a decay curve on one electrode and then the E (i) characteristic on another. Since good reproducibility cannot be guaranteed with PTFE bonded electrodes, the approach adopted was to make several successive determination of the E (i) curve sufficiently rapidly to display the pattern of the activity change with time. This necessitated the use of a slow potential sweep method. After preanodization the electrode was subjected to a 100 mv/min potential sweep between 1000 mv and 400 mv. A complete curve of increasing and decreasing potential could then be obtained in about ten minutes. The sweeps were continued until the pattern of increase and decrease in current at a particular potential was observed; the tabulated values represent the highest observed activity. A careful comparison was made of the manual and sweep method to ensure that the E (i) curves were equivalent.

E. Electrochemical Testing of Ni Plaque

Activity measurements were also made on porous nickel plaques carbided by the Bureau of Mines (#28C). The three preliminary experiments conducted on porous nickel were with an inducted carbide sample (petroleum ether to methanol sequence), an uninducted carbide sample, and the untreated nickel plaque from which the carbide samples were prepared. These samples were coated lightly on one surface with PTFE dispersion using a brush. The electrodes were heated at 275° C for five minutes in N_2, to drive off the wetting agent associated with the PTFE dispersion, and tested as floating electrodes with the PTFE treated surface in contact with the gas phase. Plaques impregnated with a dilute dispersion of PTFE resulted in a completely waterproof structure, of very low activity. The results are presented in Table V, p. 17. A third electrode was tested without any pretreatment with PTFE (#28C iii). We intend to test these electrodes in a matrix electrolyte fuel cell configuration in which the gas pressure and thus the degree of wetting of the electrode can be controlled.

III. PHYSICAL CHARACTERIZATION

An exploratory comparison was made between a nickel carbide prepared from the Raney metal and one made by decomposition of nickel acetate in terms of bulk density and pore volume distribution. Debye-Scherrer X-ray measurements were also made to confirm that they were essentially the same materials.

The bulk density of the Raney carbide, at 1.7 to 1.9 g/cm^3, was more than twice the figure for the material produced by acetate-decomposition, 0.69 to 0.93 g/cm^3. (The significance of bulk density in electrode performance was discussed in the Introduction.) The pore volume distribution for the two samples is shown in Figs.7 and 8. The two samples do not show any great difference in pore size distribution, though the Raney carbide has the greater cumulative pore volume. It is probable that the measured pore volume in the range < 100 Å makes a very small contribution to the total volume of the catalyst flooded with electrolyte. Most of the differences which exist between the two catalysts must occur in terms of pore sizes > 300 Å (a range that cannot be measured with precision by N_2 condensation) and are therefore better expressed in terms of bulk density.

The X-ray powder photographs are shown in Fig. 9. The samples are essentially the same, with two minor differences. The first is that the sample from the acetate #53 contains substantially more free nickel; the second is that the line broadening of the Bureau of Mines' sample indicates a very much smaller crystallite size for the Ni_3C.

IV. RESULTS AND DISCUSSION

The test results on catalysts prepared from Raney metals are presented in Tables II, III, IV, and VI, pp. 12 to 18 . Comparing the results obtained with the Raney metals (Table VI) to the carbides, etc., derived from them (Tables II, III, IV), it is apparent that the carbiding process adversely affects the performance. For example with the 3 Ni/Co alloy the current density at 750 mv is 32 ma/cm^2; for the carbide of this alloy the best figure observed was 24 ma/cm^2. The loss of performance is probably related to sintering of the Raney alloy during the carbiding process. The effect is further emphasized with the nitrocarbide of the 3 Ni/Co alloy, which was subject to further high temperature treatment during the nitriding process. In this case the current density fell to 18 ma/cm^2 at 750 mv. The pattern of activity of the nickel/cobalt alloys is 3 Ni/Co > Ni/Co > Ni/3Co for both the Raney alloys and the carbides; for the nitrocarbide the order was Ni/Co > 3 Ni/Co > Ni/3Co. The higher activity of the 3 Ni/Co alloy and carbide is probably due to the formation of a surface spinel, with improved conductivity and possibly enhanced catalytic activity.

The Raney alloys of nickel and silver demonstrated activities of 26 ma/cm^2 at 750 mv for the 3 Ni/Ag, and 4 ma/cm^2 at 750 mv for Ni/Ag. Both figures are very much lower than what might be expected from the known intrinsic activity of this alloy(6). This is an indication of the unfavorable physical structure of these Raney alloys for PTFE-bonded electrodes.

Towards the end of the tests reported here, the performance of the certain electrodes was examined as a function of time; the results are shown in Figs. 1, 2, and 3. The rates of decay were not identical for the three electrodes but did show the same pattern of activity: an initial increase in current, a short plateau, and then a steady decay. The normal procedure for determining an E (i) curve was to obtain points at 50 mv intervals in the potential sequence 850 mv $\rightarrow$ 400 mv $\rightarrow$ 850 mv. The results (Tables I - VI, pp. 12-18) show very different results for decreasing and increasing potentials.

Measured in that sequence the increasing potential result is larger or smaller than the former, depending on whether the first result was made on or before the plateau. Until the time variation of the current was established, the results were very confusing. The later results for which the slow potential sweep was used, as described in Part 1, section II, give the plateau values unambiguously. At this stage of the study it is considered legitimate to quote the plateau values (i. e. the maximum activity) on the basis that the conditions giving rise to this activity can be stabilized.

A possible explanation of the process is that initially, in addition to the cathodic reduction of O_2, there is a simultaneous anodic process associated with further oxidation of the surface. This falls rapidly to a low value when the surface is completely covered and produces an apparent increase in the net cathodic current. The oxygen reduction process is assumed to occur on the oxide surface and not on the bare metal. However, it is surprising that the surface oxidation is not complete during pretreatment of these electrodes at 1600 mv for 10 min. The decay process that was then observed may be related to an increase in the resistance of the electrode. The operation of PTFE bonded electrodes depends on good electrical conductivity between individual catalyst particles and since conductivity of the oxide is considerably lower than that of the metal, the electrode resistance increases. The points or faces of contact probably oxidize more slowly than the exposed surfaces, so that this process would not be complete within the time span of the surface oxidation responsible for the apparent increase in current described above.

The above argument suggests that some of the iR corrections made to the earlier results might be too large. The ohmic resistance was measured by the interrupter technique (resolution time 0. 2 μsec.). The over-all resistance measured for the nickel and nickel cobalt electrodes are approximately twice that measured with a Pt electrode, indicating a significant contribution from the resistance of the electrode. This electrode resistance, in contrast to the bulk electrolyte resistance, is inevitable in the practical operation of the electrode and may not be a valid experimental correction of the E (i) curve. In the future only the electrolyte correction will be used (i. e. the figure obtained for a Pt electrode with the same distance between the working electrode and the reference electrode). The over-correction, about 0.6 Ω or 60 mv at 100 ma/cm^2, is important only for those electrodes with high activity.

It is intended to examine the changes of resistance with time on an active electrode to check that the pattern coincides with the activity time curve. Comparison of the behavior of catalysts prepared from Raney alloys and from decomposition of acetate,with regard to decay and resistance change, will also be made.

Fifteen samples of Ni_3C were prepared by acetate decomposition in the laboratory and from these, twenty-four electrodes were made for testing; the results are presented in Table I, p. 12 . Eight of these electrodes showed an activity better than 12 ma/cm^2 at 750 mv. The best examples are 53 (i)b: 44 ma/cm^2, 62 (i): 40 ma/cm^2, and 63 (ii): 100 ma/cm^2. The last three electrodes all showed a limiting current > 250 ma/cm^2 at 600 mv, Figs. 4, 5, and 6. No explanation can be offered for the wide range of activities observed for electrodes and catalysts prepared and tested in an apparently identical manner. Where variations do exist in terms of the catalyst preparation, method of induction, or electrode fabrication, no logical pattern was observed. It is possible that in the preparation of the catalysts the position of the sample in the furnace or the gas flow rate may be critical; these factors have not been rigidly controlled. This method of preparation is being attempted by the Bureau of Mines under more controlled conditions. More detailed examined of Ni_3C is intended, particularly with regard to physical characterization of the catalyst and electrode structure.

According to the limited data available at this time, the rate of decay of electrodes made from acetate-decomposition catalysts is slower than those made from Raney alloy based catalysts. This could be related to the possibility of larger sized agglomerates in the former (see section III), since extensive agglomeration should result in a slower breakdown of the conductive paths in the electrode.

The primary conclusion to be made from the results presented in this report is that the Raney catalysts before and after carbiding or nitriding did not show an activity comparable with the best observed for Ni_3C prepared by acetate decomposition. This is attributed to physical differences in the two sources of catalyst which influence the operating characteristics of PTFE bonded electrodes. The best result obtained from Ni_3C by acetate decomposition was 100 ma/cm^2 at 750 mv and a limiting current > 250 ma/cm^2 at 600 mv. For Ni_3C prepared from Raney nickel, the corresponding figures were 37 ma/cm^2 and 94 ma/cm^2. The tests on the other materials – the Raney alloys, carbides, and nitro-carbides in this series – were less extensive than those on Ni_3C and probably do not represent the best performance that could be obtained. However, we believe that the tests accurately describe the relative over-all activities of these materials but do not necessarily give a good measure of the intrinsic activity because of the effect of electrode structure.

TABLE I

Activity of Ni_3C Prepared by Acetate Decomposition

Catalyst Preparation (1)				Electrode (2)		
					Activity ma/cm² (3)	
Sample	Time hrs.	Temperature °C	Induction	Loading mg/cm²	at 750 mv	at 600 mv
49(i)(4)	3.0	300	No	26	5/3	8/7.5
49(ii)			No	11	1.4/-	2.7/-
50	3.5	300	No	13	1.1/-	2.0/-
51	4.0	300	No	37	0.1/-	0.4/-
52	1.5	300	No	18	1.2/-	1.3/-
53(i)a	3.0	300	No	27	8/14	96/36
53(i)b			No	30	44/30	$i_L > 250$ ma/cm²
53(i)c			No	19	---	69/2.6
53(ii)	3.0	300	No	22	4.6/-	1.2/-
54(5)	3.0		No	27	1.4/-	48/-
55	3.0	350	No	43	8/12	41.47
55			No	44	16/20	87/75
56	3.0	300	No	11	6/1.2	9.8/2.9
56			No	9	18/9	58/30
57	3.0	300	No	32	0.3/-	0.7/-

(Footnotes on following page)

TABLE I (Cont.)

Catalyst Preparation[1]				Electrode[2]		
					Activity ma/cm^2 [3]	
Sample	Time hrs.	Temperature °C	Induction	Loading mg/cm^2	at 750 mv	at 600 mv
58	3	300	Yes	28.4	7/30	125/104
59	3	300	Yes	22.6	16/3	82/3.5
60	9	300	No	27.8	5	11/3.5
61	4	300	No	28.9	7.5/1.5	13.0/5.0
62(i)[4]	3	300	No	27.4	40/2	$i_L > 250$ see Fig. 5
62(ii)			No	33.7	10/0.5	18/0.1
62(iii)			Yes	16.3	9/0.5	50/1.5
63(i)	3	300	No	24.3	8/9	51/25
63(ii)			Yes	9.76	100/8	$i_L > 250$ see Fig. 6

(1) All preparations from 1.5g partially dehydrated nickel acetate, except #49, 50, 51 from $Ni(C_2H_3O_2)_2 \cdot 4\,H_2O$

(2) All electrodes contained 20% PTFE and were sintered for 5 min. at 275°C, except 49(ii) & 50, 30% PTFE and 49(ii) sintered 10 mins. and 49(i) and 57 sintered 15 mins.

(3) Expressed as decreasing potential value/increasing potential value.

(4) Numbers in italics indicate separate electrodes made from the same catalyst preparation.

(5) Prepared by heating successively at 200°C for 3 hr., 275°C for 4 hr., 300°C for 4 hr. and further 300°C for 1 hr. No color change until 300°C treatment, no change in activity after further heating.

TABLE II Activity of Bureau of Mines Catalysts

	Electrode Preparation						Activity(1)	
	Electrode	Induction	%PTFE	Sintering Temp. ° C.	Sintering Time-Min.	Loading mg/cm^2	ma/cm^2 at 750 mv.	ma/cm^2 at 600 mv.
Co_2C	#20C(i)	Yes	10	275	5	35.5	0.4/0.4	0.8/1.0
	#20C(ii)	No	10	275	5	57.4	10/9	43/35
$Ni/_{Co}C$	#25C(i)a	Yes	20	275	5	60.4	16/2	43/6
	#25C(ii)a	No	20	275	5	49.5	6/2	19/6
$Ni/_{3Co}C$	#26C(i)a	No	30	275	5	45.5	12/6	28/15
	#26C(i)b	No	30	275	5	41	6/10	16/23
	#26C(ii)a	Yes	30	275	5	55	4/a (2)	11/2
	#26C(iii)a	No	20	275	5	56	7/a	13/1
	#26C(iv)a	Yes	20	275	6	61	a/a	18/2
	#26C(iv)b	Yes	20	275	5	39	7/0.3	16/1
$3Ni/_{Co}C$	#27C(i)a	Yes	20	275	5	46.7	24/24	72/72(3)
	#27C(i)b	Yes	20	275	5	51.4	14/15	44/44
	#27C(ii)a	No	20	275	5	63.4	13/14	36/40
	#27C(ii)b	No	20	275	5	45.1	14/13	34/34

(1) Expressed as decreasing potential value/increasing potential value

(2) a - Anodic current

(3) Results of 100 mv/min sweep for this and succeeding measurements

TABLE III Activity of Bureau of Mines Catalysts

	Electrode Preparation						Activity (1)	
	Electrode	Induction	% PTFE	Sintering Temp. °C.	Sintering Time, Min.	Loading mg/cm^2	ma/cm^2 at 750 mv.	ma/cm^2 at 600 mv.
Ni_3NC	#11NC(i)	Yes	20	275	5	45.4	8/1.5	23/5
	#11NC(ii)	No	20	275	5	57.4	10/9	43/35
Co_2NC	#12NC(i)	No	10	275	5	45.5	0.1	0.7
	#12NC(ii)	Yes	10	275	5	37	0.2	0.5
$Ni/_{3Co}NC$								
	#13NC(i)a	Yes	30	275	5	-	not tested	
	#13NC(ii)a	Yes	30	275	5	-	not tested	
	#13NC(iii)a	No	20	275	5	45	a/5	49/12
	#13NC(iv)a	Yes	20	275	5	50	10/a	27/1
$3Ni/_{Co}NC$								
	#15NC(i)a	Yes	20	275	5	56.4	14/11	33/28 (2)
	#15NC(i)b	Yes	20	275	5	-	corrosion test	
	#15NC(ii)a	No	20	275	5	49.2	18/16	44/42
$Ni/_{Co}NC$								
	#16NC(i)a	Yes	20	275	5	49.7	11/13	37/27
	#16NC(ii)a	No	20	275	5	53.2	25/22.5	68/68

(1) Activity expressed as decreasing potential value/increasing potential value

(2) Potential sweep of 100 mv/min used for this and succeeding measurements.

TABLE IV Activity of Bureau of Mines Catalysts

Electrode Preparation						Activity [(1)]	
Electrode	Induction	% PTFE	Sintering Temp. °C.	Sintering Time, Min.	Loading mg/cm^2	ma/cm^2 at 750 mv.	ma/cm^2 at 600 mv.
#19C(i), Ni_3C	Yes	20	275	15	51	-/4	21/14
#19C(ii), Ni_3C	No	20	275	15	49	-/3.5	46/18
#19C(iii), Ni_3C	No	10	275	5	68	13/2.5	19/7
#19C(iv), Ni_3C	No	20	275	5	48	14/10	55/29
#19C(v), Ni_3C	No	15	275	5	60	37/14	94/44
#19C(vi), Ni_3C	No	10	275	5	79	16/8	38/18
#19C(vii), Ni_3C	No	15	275	5	58	20/9	69/38

(1) Activity expressed as decreasing potential value/increasing potential value

TABLE V Activity of Carbided Nickel Plaques

Sample	Induction	Electrode Preparation	Activity ma/cm^2 at 750 mv.	Activity ma/cm^2 at 600 mv.
28 C (i)	PET	PTFE Brushed	1.2/12[(1)]	5/19
28 C (ii)	None	PTFE Brushed	1.8/7.2	5/8.4
28 C (iii)	None	None	0.3/0.6	0.7/1.1
Pure Ni	None	PTFE Brushed	0.9/2.9	3.8/10.8

(1) Activity expressed as decreasing potential value/ increasing potential value

TABLE VI Activity of Bureau of Mines Catalysts

	Electrode Preparation						Activity (1)	
	Electrode	Induction	% PTFE	Sintering Temp. °C.	Sintering Time, Min.	Loading mg/cm^2	ma/cm^2 at 750 mv.	ma/cm^2 at 600 mv.
Ni/Co	RAL 1 (i)a	No	20	275	5	37.0	17/2	5/5.6 (2)
Ni/3Co	RAL 2 (i)a	No	20	275	5	45.2	13/12	2.6/3.2
3Ni/Co	RAL 3 (i)a	No	40	275	5	36.0	32/36	60/64
Ni/3Ag	RAL 4 (i)a	No	20	275	5	46.3	26/26	76/84
Ni/Ag	RAL 5 (i)a	No	20	275	5	35.9	4/4	12/30

(1) Activity expressed as decreasing potential value/increasing potential value

(2) All measurements using 100 mv/min potential sweep.

PART 2(a)

GOLD PALLADIUM ALLOYS

I. INTRODUCTION

Previous measurements on gold alloys of Pt, Pd, and Ag showed the Au/Pd alloys to have the highest activity for O_2 reduction. Furthermore, this high activity (higher than pure Pt and pure Pd)* extended over a wide range of alloy composition from 20 to 70% gold. The high activity of the gold rich alloys is particularly encouraging since these alloys are more corrosion resistant than pure Pd. Pure Pd is active for O_2 reduction but does not show the corrosion free behavior of pure Pt.

Accordingly, we have set out to prepare Au/Pd alloys in highly dispersed form (blacks) for testing as PTFE bonded electrodes.

* Further data confirming this effect at 25 and 75°C and the current distribution on the face and sides of the rotating cylindrical electrode are included in this report, Figs. 10, 11, and 12. This completes the study described in detail in the Sixth Quarterly Report.

II. EXPERIMENTAL

We selected formaldehyde reduction of a solution of $HAuCl_4$ and $PdCl_2$ for preparation of the black. This reaction avoids the complications of the widely used borohydride reduction, which has two disadvantages: the possible introduction of boron into the product and the difficulty of predicting the composition of the product. The formaldehyde reduction has been used extensively at Tyco for the preparation of Pt blacks in a reproducible manner. The key to reproducibility is the control of the nucleation and mixing stages of the preparation. The method is based on the work of Turkevich, Hillier and Stevenson[7] and has been described in detail elsewhere[8]. Briefly, precipitation occurs in strongly alkaline solution by an electrochemical mechanism on preformed nuclei in solution; formaldehyde is oxidized at one site and the metal ion is reduced at another site on any given nucleus. The formation of nuclei, a slower molecular reaction, can be induced at lower pH where the rate of the electrochemical process is negligible. By separating the nucleation step and the growth (electrochemical) process by adjusting the pH, a more uniform product can be prepared.

The experimental procedure was to take a portion (1/4) of the gold palladium solution (6.160 g of $HAuCl_4$ and 6.465 g of $PdCl_2$ in 475 ml of water filtered through a Millipore filter)* and add twice the stoichiometric requirement of formaldehyde followed by sufficient sodium carbonate to bring the pH to 8.5. After ten minutes, during which time (as shown for Pt) the number of nuclei has reached a constant value, this solution and the remainder of the gold palladium solution (plus formaldehyde) is added rapidly (< 2 sec) to a vigorously stirred solution of NaOH at 90°C. The precipitation of the black, including agglomeration, was complete in 3 min. Oxygen was bubbled through the system during the reaction and for ten minutes afterwards. The black was collected, washed free from sodium chloride, and allowed to dry in air.

---

* All solutions were passed through a Millipore filter capable of removing particles down to 0.2 μ; this reduced the possibility of heterogeneous nucleation, a source of irreproducibility.

III. RESULTS

One black was prepared and tested in which the ratio of Pd to Au in the starting solution was 70:30. X-ray measurements, gave the gold content of the alloy black as 27%.

Electrodes were made with 20 and 30% PTFE content. These are compared with a Pt electrode made in a similar manner in Figs. 13 and 13a. At low polarization the Au/Pd catalyst in an electrode with 20% PTFE is more active than Pt; at 950 mv the Au/Pd electrode produced 60 ma/cm^2 compared with 32 ma/cm^2 for Pt.

PART 2(b)

SOLID ELECTRODES – TITANIUM, TITANIUM DIOXIDE, AND RELATED INTERMETALLIC COMPOUNDS

I. INTRODUCTION

In a previous quarterly report(9) it was noted that the intermetallic compound Ti_3Au showed considerable catalytic activity for the reduction of oxygen, though it was subject to some corrosion. However, when attempts were made to run a powdered form of Ti_3Au as a floating electrode, they were unsuccessful because of oxidation of the catalyst to a nonconductive state.

It has been suggested that the activity of the Ti_3Au intermetallic in solid form may be due to the formation of a nonstoichiometric phase of titanium dioxide by the chemical and/or electrochemical environment to which it is subjected in testing. The nonstoichiometric form is characterized by having a conductivity ($TiO_{1.75} = 10^2\ \Omega^{-1}cm^{-1}$) that is much greater than TiO_2 ($10^{-10}\ \Omega^{-1}cm^{-1}$)(10). Therefore, since the electrochemistry of pure gold is reasonably well defined, we have turned our attention to a more detailed study of the electrochemistry of titanium, and more especially nonstoichiometric titanium dioxide. The activity of pure titanium (99.9%) has been measured in the form of a cylinder mounted as a Makrides-Stern electrode(11). These measurements were made at 25°C rather than at 75°C, as previously. The results obtained agree well with previous work as well as with the data in the available literature. Details of this work are given in the next section.

Nonstoichiometric titanium dioxide is easily obtained by chemical reduction of TiO_2 and as mentioned above it exhibits varying degrees of electrical conductivity in such a reduced state. In addition it has been found, and reported in the literature(12), that "black oxide" films are formed on titanium under certain conditions in alkaline solution. Such "black oxides" are conductive and show some catalytic activity for O_2-reduction. In order to investigate this more deeply, we have decided to study the behavior of single crystals of TiO_2 for different crystallographic orientation and varying stoichiometry (easily controlled and defined for single crystals). The single crystal is also particularly interesting because the conductivity is anisotropic. Along the c-axis the conductivity is, at a particular stoichiometry, 20,000 X greater than along the a-axis. This ratio as a function of stoichiometry has been measured for the range $TiO_{1.75}$ to TiO_2 by Hollander and Castro[13]. A series of experiments is planned in which the behavior of the crystal planes parallel to and perpendicular to the c-axis will be examined for the full range of stoichiometry. The first experiment of this series is described in this report.

In addition to the work on Ti and TiO_2, the following intermetallic compounds bearing a close similarity to Ti_3Au were studied: $TiAu_2$, V_3Au, and Nb_3Au. Ti_3Au, TiAu, $TiRh_{1.5}Au_{1.5}$, and $TiRh_3$ were re-examined. The repeat measurements on the titanium compounds were carried out because the initial results showed some unusual features and because improvements have since been made in the apparatus and experimental technique. The current data, for example, has been obtained at 25°C rather than 75°C. The present results can, therefore, be more confidently compared with the results in the detailed study of titanium and its compounds.

II. EXPERIMENTAL PROCEDURES AND RESULTS

For the tests performed with titanium, it was decided that a Makrides-Stern electrode configuration would be more suitable than the "Koldmount" device used in previous tests. The cylinder of titanium was machined from (99.9%) titanium rod. Runs were made in 2N KOH at 25°C in N_2 and then O_2-saturated solution; the electrode was rotated at 600 RPM; potentials were measured vs. reversible hydrogen electrode in the same solution; H_2-charged Pd-Ag was used as counter electrode.

In the first run (Fig. 14) the usual sweep from 1000 to 0 mv at 50 mv/min was made. O_2-reduction current was first observed at 400 mv. The diffusion limited current was not reached above zero mv. The corrosion current observed under nitrogen was of the order of 10-20 $\mu a/cm^2$.

In the second run (Fig. 15) the potential sweep was extended from -600 mv to +1600 mv, and the sweep rate was increased to 1 volt/min. It can be seen in this figure that the O_2 diffusion limiting current has not reached a plateau even at -300 mv. Figure 16 shows a rerun of the sweep under N_2 on a more sensitive scale. Figures 17, 18, and 19 illustrate the effects on O_2-reduction of sweeping through different potential ranges. The reaction apparently occurs on an oxide layer down to potentials of -450 mv. The hysteresis becomes greater when the sweep is extended to -600 mv (Fig. 17), but the surface may still retain some oxide. When the sweep is extended to -900 mv or held at -600 mv, O_2-reduction is apparently taking place on a clean titanium metal surface, as indicated by the large hysteresis and the exceptionally flat diffusion current plateau (Fig. 19).

Oxide films on titanium were formed by exposing the electrode to alkaline solutions containing hydrogen peroxide. According to a paper by Bianchi, Mazza and Trasatti[15], "black oxide" formation occurs in preference to passivation or corrosion in 1N solutions of NaOH with peroxide concentrations of 0.1 to 1.0 molar. The titanium electrode was exposed in the first case to 0.1 molar peroxide solution for 120 hours. The potential (vs. RHE same solution) was recorded and the change is shown in Fig. 20. The potential rise observed should indicate, according to Bianchi, et al., that passivation rather than "black oxide" formation had occurred. The electrode, when examined, was in fact a light bluish-gray rather than black. This electrode was then tested for O_2-reduction activity; the results compared to smooth titanium are shown in Fig. 21. The potential at which O_2-reduction occurs is shifted to more positive values, and the double layer capacity is approximately doubled. An extended potential sweep is shown in Fig. 22 for comparison to Fig. 21.

In a subsequent experiment the peroxide concentration was increased to 1M. An attempt was made to follow the potential change, but measurements could not be made either because of peroxide contamination of the reference electrode or hydrogen leakage. The electrode was left in solution for 20 hours and then tested for O_2-reduction activity. It had a heavy, adherent black film on its surface. The results are shown in Fig. 23 in comparison again to smooth titanium. The shift in potential for O_2-reduction is significantly more positive and the double layer capacity increased by a factor of 25.

Titanium powder was exposed to 2N KOH at 100°C for five hours and then allowed to cool in the solution for ~ 15 hours. These are the conditions under which Ti_3Au formed a nonconductive (200,000 ohms), black powder, as reported previously[16]. The bluish-black powder obtained from titanium presently has a resistance of ~ 50 ohms. This material was made into a Teflon-bonded electrode and operated as a floating electrode in 35% KOH at 75°C. Activity for O_2-reduction was not discernible, the behavior being similar to that of the black Ti_3Au. A second sample of titanium powder was exposed to the same solution (1.0M KOH, 1.0M H_2O_2) for 120 hours. A light bluish-black powder was obtained and was tested as a PTFE bonded electrode in 35% KOH at 75°C; again there was no measurable activity.

For the experiments with the single crystal of TiO_2, a rutile boule was bought from the National Lead Company. Its crystallographic orientation was determined using the Laue X-ray diffraction method, prior to cutting into small samples 3/8" square and 3/16" thick for testing as rotating electrodes. Two samples were prepared with the working face perpendicular to the c-axis,

(001) plane, and two with the working face perpendicular to the a-axis, (010) plane. The boule as received was blue and translucent, indicating that it was in a partially reduced (nonstoichiometric) state. The first tests were carried out on the as-received crystals for which the specific resistivity was measured as 23 Ω-cm.

In view of the marked anisotropy of conductivity, it was difficult to make good electrical contact with the sample in the Koldmount rotating electrode structure. For the crystal with the working face perpendicular to the c-axis, a point or ring contact was soon demonstrated to be insufficient because of the low conductivity parallel to the plane of the contact face. The first approach was to vapor plate gold on to the face of the crystal opposite to the working face. However, it was found that the contact point broke through the gold film on assembly, and no real reduction in contact resistance was achieved. Good contact was eventually made when the gold was protected by a conducting silver-epoxy cement. (The vapor plated gold was retained in addition to the silver cement in order to be able to remove the epoxy cement from the crystal at the end of the experimental measurements. This is essential since the crystal is to be reduced at 800-1000°C in hydrogen(17), conditions under which decomposition of the epoxy cement would take place with possible contamination of the crystal.)

The results obtained so far are presented in Figs. 24 and 25. The stoichiometry of the crystals in these preliminary measurements is not known*, but it would appear from the electrochemical behavior that it is close to TiO_2. Interesting differences are already apparent between the two crystallographic orientations. The potential at which a reduction current is first discernible (E_i) is 100 mv greater for the c-axis crystal (at 375 mv vs. RHE) than for the a-axis crystal. The effect of the difference in conductivity can be seen in the less rapid increase of current with potential for the a-axis crystal below 275 mv. The crystals are at present being reduced in H_2 at 1000°C, conditions under which the stoichiometry is a function of time for further electrochemical tests.

* In future experiments the stoichiometry will be determined gravimetrically by reoxidation to TiO_2.

The intermetallic compounds related to Ti_3Au that were examined are described below:

A. $TiAu_2$

This material, a brittle intermetallic compound, was tested as a Koldmount formed rotating disc electrode in 2N KOH at 25° C. The results are presented in Fig. 26.

B. TiAu

The test conditions were as for $TiAu_2$ above; the results are presented in Fig. 27. This material was tested previously but at 75° C. The experiment was repeated since the initial results (Fig. 28) showed significant activity with a much reduced corrosion rate compared with TiAu; this needed confirmation. Also, with the improvements made on the apparatus since these measurements were made and the temperature modification, it was desired to put the previous results on Ti compounds on the same basis as the present ones. A comparison of the results is given in Table VII.

C. $TiRh_{1.5}Au_{1.5}$

The test conditions were as for $TiAu_2$ above, the results are presented in Fig. 29, and the previous measurement is shown in Fig. 30 for qualitative comparison (75° C vs. 25° C).

D. $TiRh_3$

This material was tested as $TiAu_2$ above; the present and previous results (75° C) are presented in Figs. 31 and 32, respectively.

E. V_3Au and Nb_3Au

These materials were tested as Koldmount formed rotating disc electrodes in order to compare their behavior with Ti_3Au. The results are presented in Figs. 33 and 34.

F. Ti_3Au

A sample of Ti_3Au was rerun to look for any change in the current voltage characteristic with the improved experimental technique. The

TABLE VII

Activity of Titanium and Related Intermetallic Compounds

	$E_{1/2}$(mv) (1)	E_i (mv) (2)	$i_L(\mu A/cm^2$	Capacity $\mu F/cm^2$	Corrosion
Ti_3Au	810	910	698	69.8	some corrosion
Ti_3Au*	840	900	1050	164.	particularly > 800 mv
TiAu	745	925	746	50.7	
TiAu*	800	860	833	56.7	
$TiAu_2$	725	800	665	46.8	some corrosion >700 mv
$TiRh_{1.5}Au_{1.5}$	825	920	658	225.	v. small
$TiRh^*_{1.5}Au^*_{1.5}$	570(3)	790	1296	109.	v. small
$TiPt^*_3$	820	870	882	132.	"
$TiRh_3$	610	920	1266	129.	"
$TiRh^*_3$	460	670	1333	116.	"
V_3Au		Corrodes rapidly for E= 400 mv			
Nb_3Au	(825)	(910)	582	-	significant corrosion rate
Pt^*	845	925	1350	115.	
Au	785	900	1340	96.	
Rh	544	675	1370	340.	

* Previous measurements (at 75° C)

(1) $E_{1/2}$ - half wave potential

(2) E_i - potential at which initial cathodic current observed

(3) Low $E_{1/2}$ value due to high anodic starting potential forming a thick oxygen film not completely removed during the initial part of the potential sweep.

results are summarized in Table VII and Figs. 35 and 36, including earlier work at 75°C. The activity is lower at lower temperature, as expected, except for Ti($Rh_{1.5}Au_{1.5}$) which now shows a half wave potential ($E_{1/2}$) 355 mv more positive

Comparing the experimental curves it can be seen that considerable hysteresis occurred in the initial measurements and that this is not reproduced in the present results. It is difficult to explain the difference in behavior in terms of temperature change. This difference could be due to more positive starting potentials of the earlier measurements producing an oxide film that is more difficult to remove.

The practice of tabulating the results of the potential sweep from positive to negative potentials (i.e. those obtained on an oxidized rather than a reduced surface) resulted in a very low value of $E_{1/2}$ being recorded. The present results are very close to those of $TiPt_3$. As described in the Fifth Quarterly Report, the Rh/Au combination can be regarded as a "synthetic" platinum in terms of electronic structure. The comparison is made in terms of the Ti intermetallic compounds because Rh and Au are not mutually soluble to any great extent.

The $TiRh_3$ sample also showed less hysteresis than the previous curve so that as with the $TiRh_{1.5}Au_{1.5}$ the $E_{1/2}$ value is higher by 150 mv. Again the hysteresis can be attributed to the more positive starting potential of the earlier results. $TiAu_2$ shows the same corrosion resistance as TiAu but the increased gold content results in a lowering of the activity. $TiAu_2$ ($E_{1/2}$ = 725 mv); TiAu ($E_{1/2}$ = 745 mv). Both V_3Au and Nb_3Au showed rapid corrosion rates, the vanadium compound particularly at potentials > 400 mv.

Limiting currents are listed as a guide to whether the over-all process is $O_2 \rightarrow H_2O_2$ or $O_2 \rightarrow H_2O$, ($i_{LH_2O} \approx 2 \times i_{LH_2O_2}$). The double layer capacity is a measure of the surface roughness of the electrode.

REFERENCES

1. Sixth Quarterly Report, Contract No. NASW-1233, December, 1966.

2. J. Giner and S. Smith, Electrochem. Technology, 5, 61 (1967).

3. J. Giner, J. Electrochem. Soc., 111, 376 (1964).

4. G. Fenillade, Proceedings of International Meeting on Fuel Cells, Brussels (organized by SERAI), Vol. IV, page 49.

5. Fifth Quarterly Report, NASW-1233, September, 1966.

6. J. M. Auclair, Proceedings of International Meeting on Fuel Cells, Brussels (organized by SERAI), Vol. II, page 45.

7. J. Turkevich, J. Hillier, and P. C. Stevenson, Disc. Far. Soc., 11, 55 (1951).

8. Final Report, Contract No. DA 44-009-AMC-410 (T), January, 1967.

9. Final Report, Contract No. NASW-1233, June1960.

10. Gmelins Handbuch, Part 41, p. 214, Weinheim 1951.

11. M. Stern, A. C. Makrides, J. Electrochem. Soc., 107, 782 (1960).

12. A. Bianchi, F. Mazza, and S. Trasatti, Proc. Second Intn'l Congress on Metallic Corrosion, p. 106, N. Y. 1966.

13. L. E. Hollander and P. L. Castro, Phys. Rev. 119, 1882 (1960).

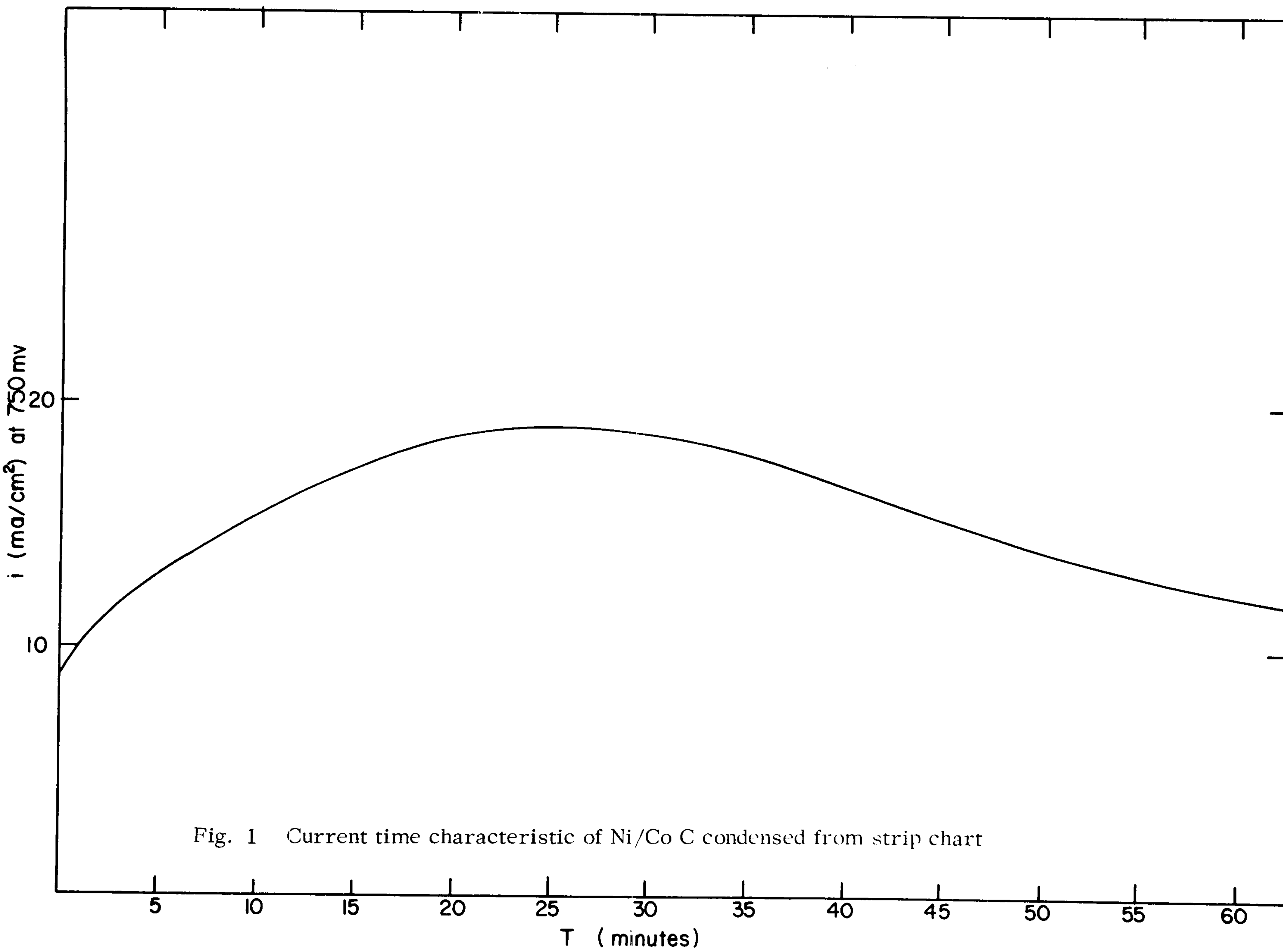

Fig. 1 Current time characteristic of Ni/Co C condensed from strip chart

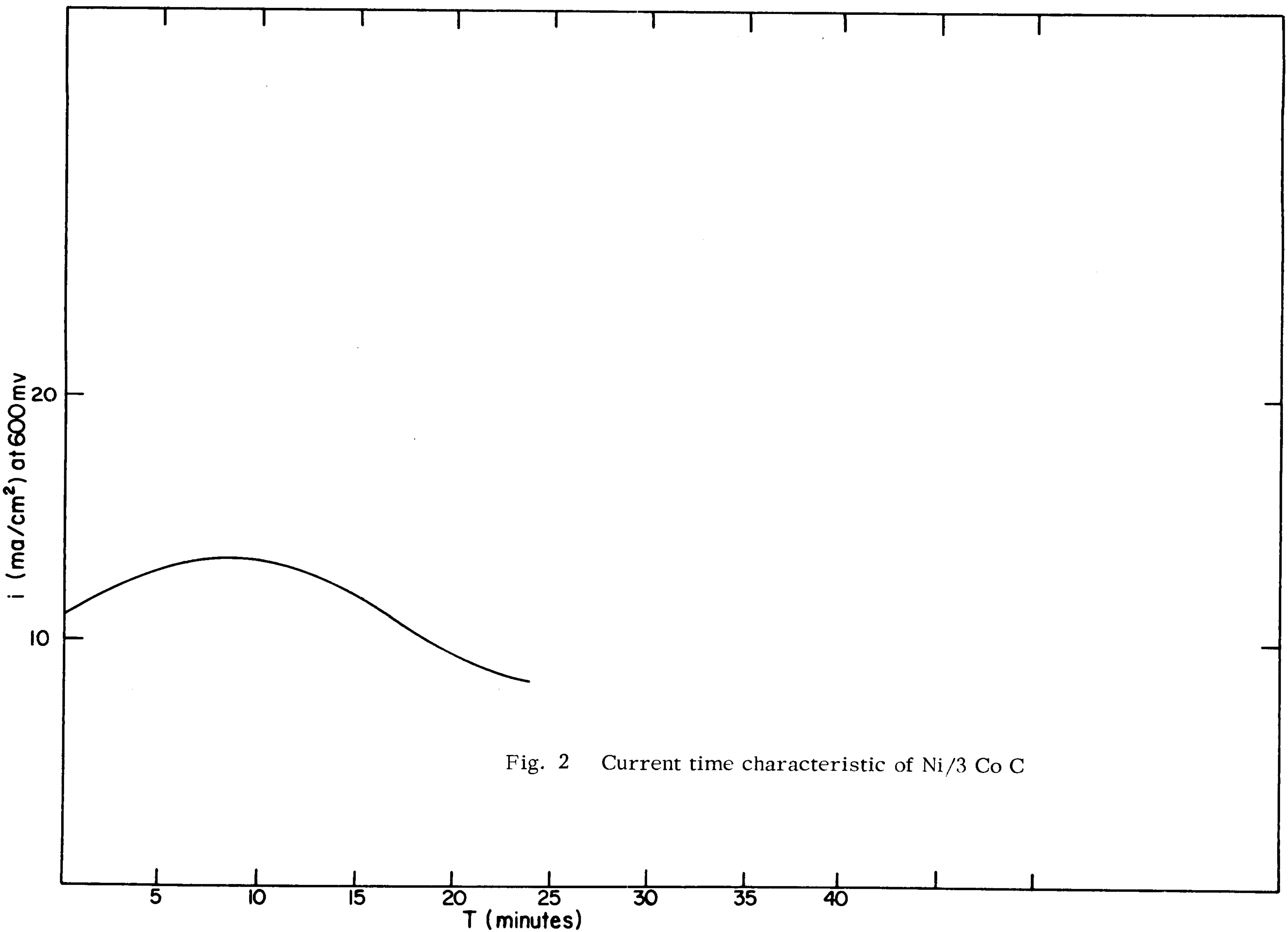

Fig. 2 Current time characteristic of Ni/3 Co C

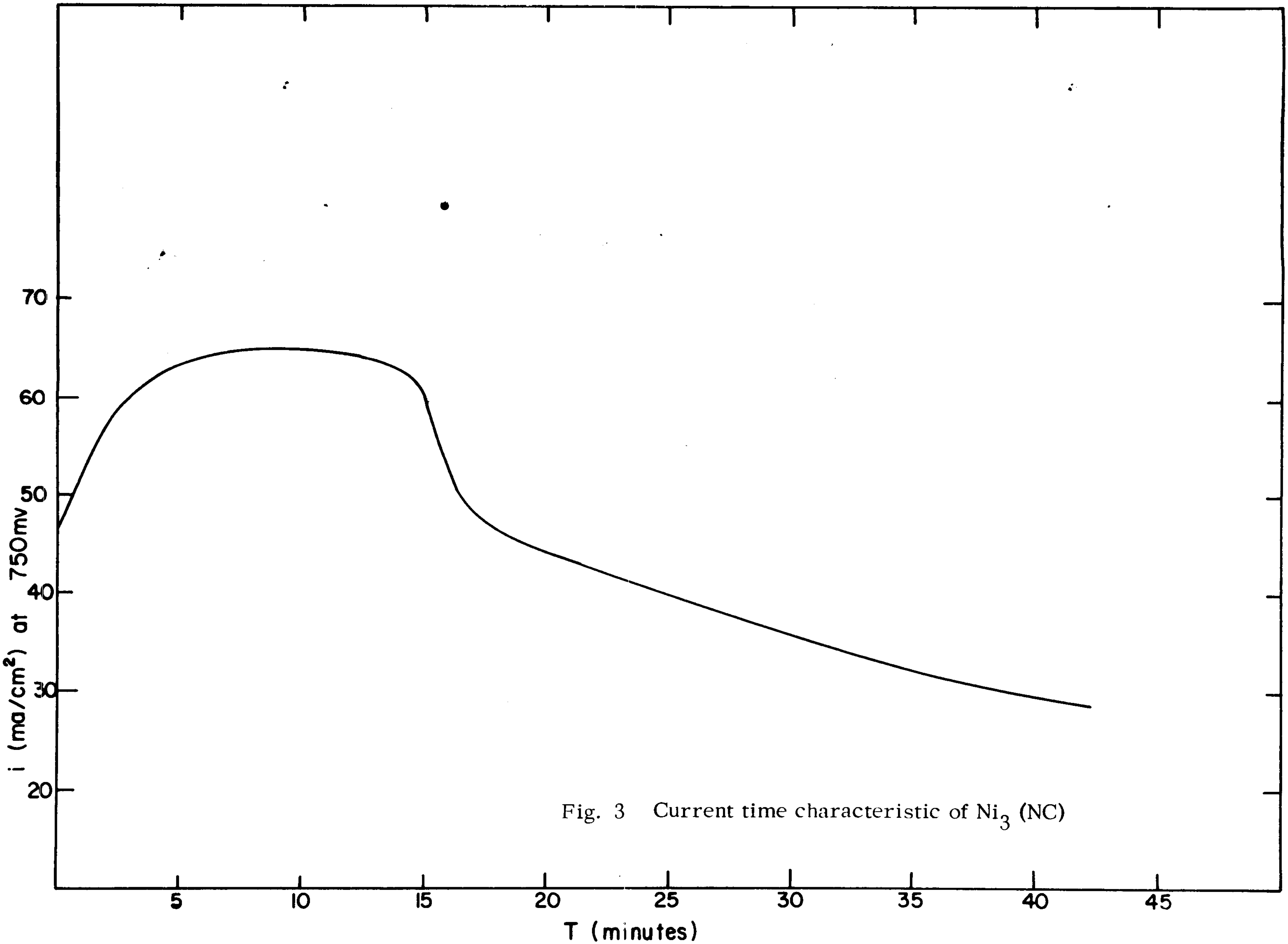

Fig. 3 Current time characteristic of Ni_3 (NC)

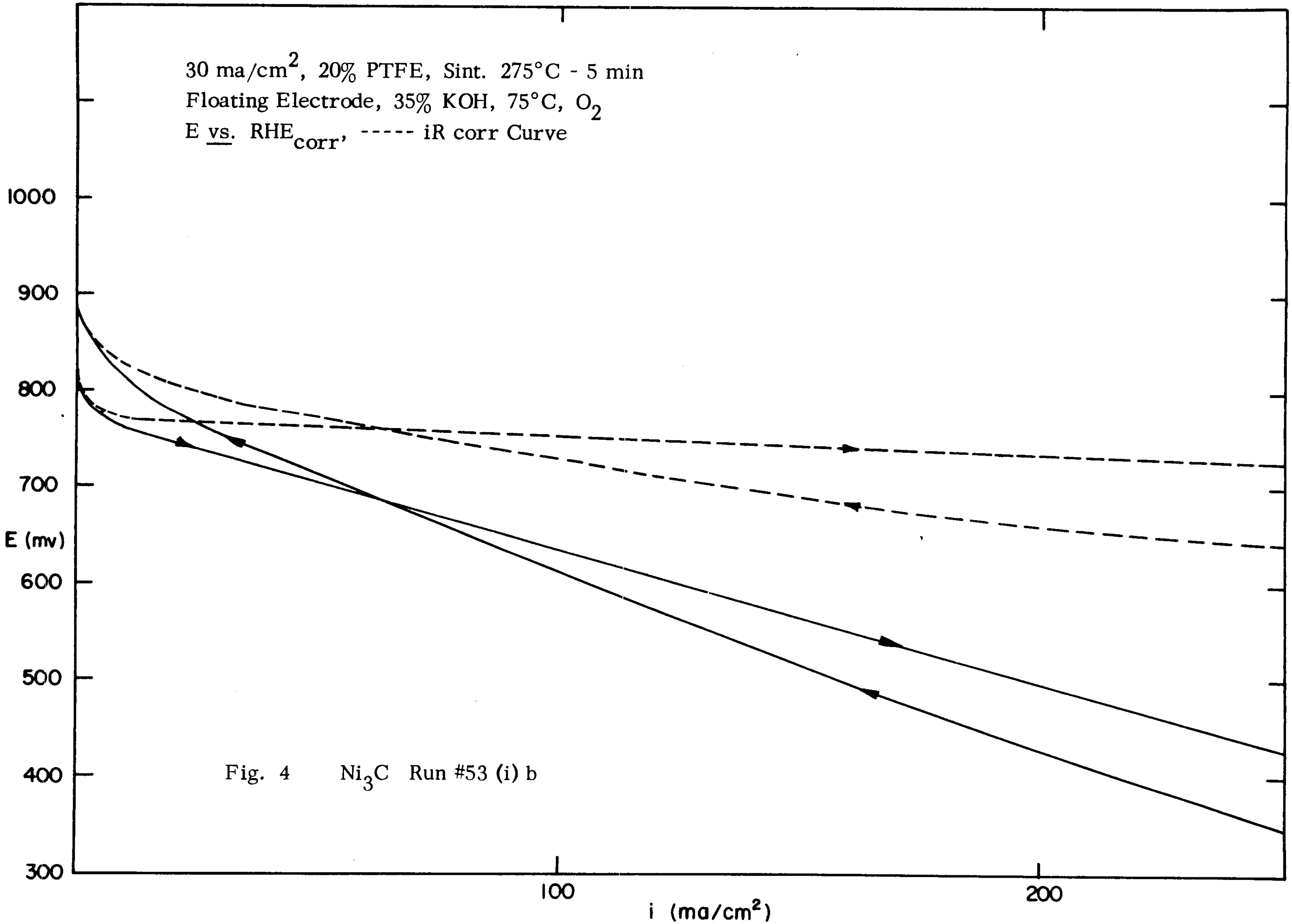

Fig. 4 Ni_3C Run #53 (i) b

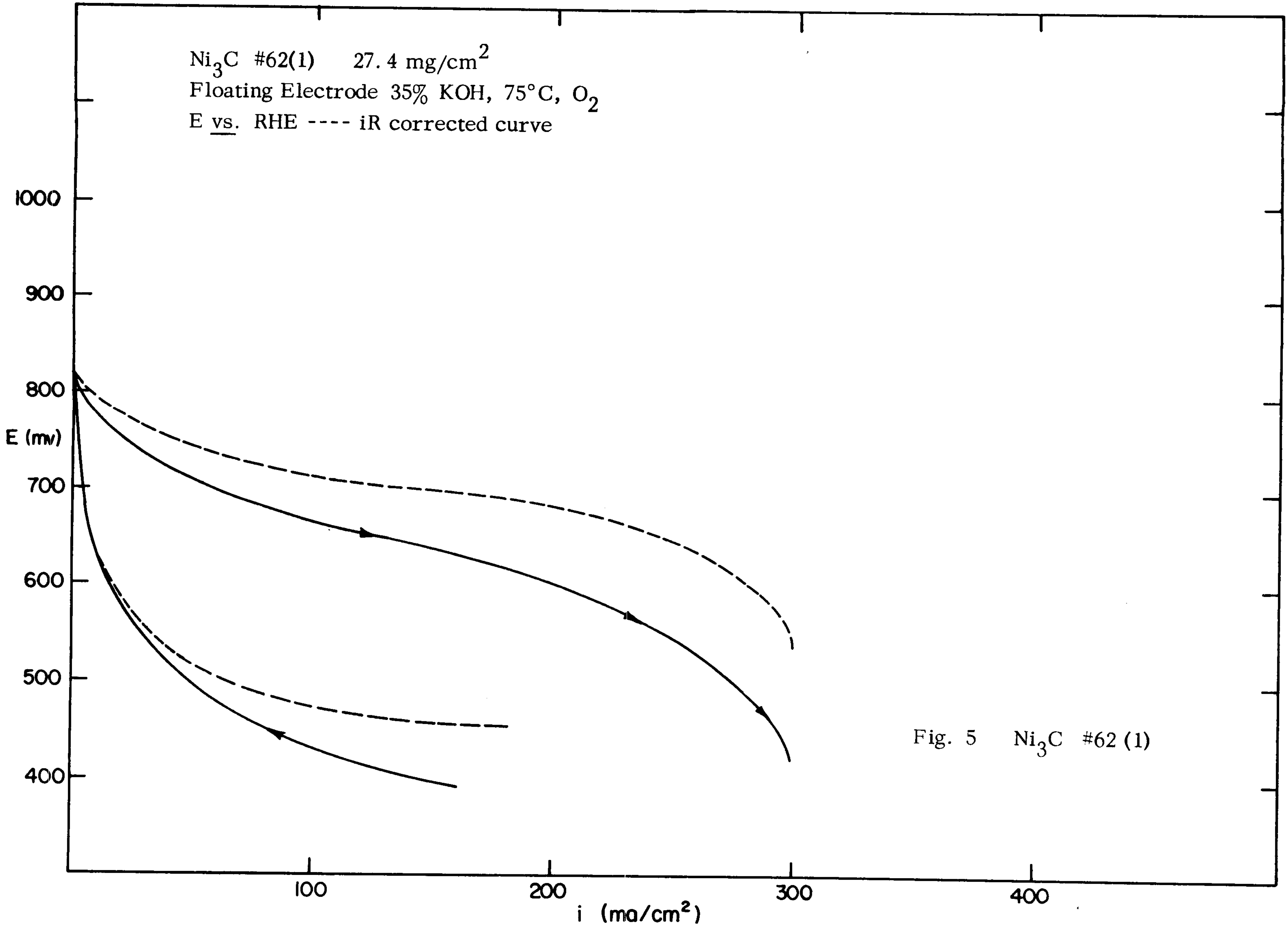

Fig. 5 Ni_3C #62 (1)

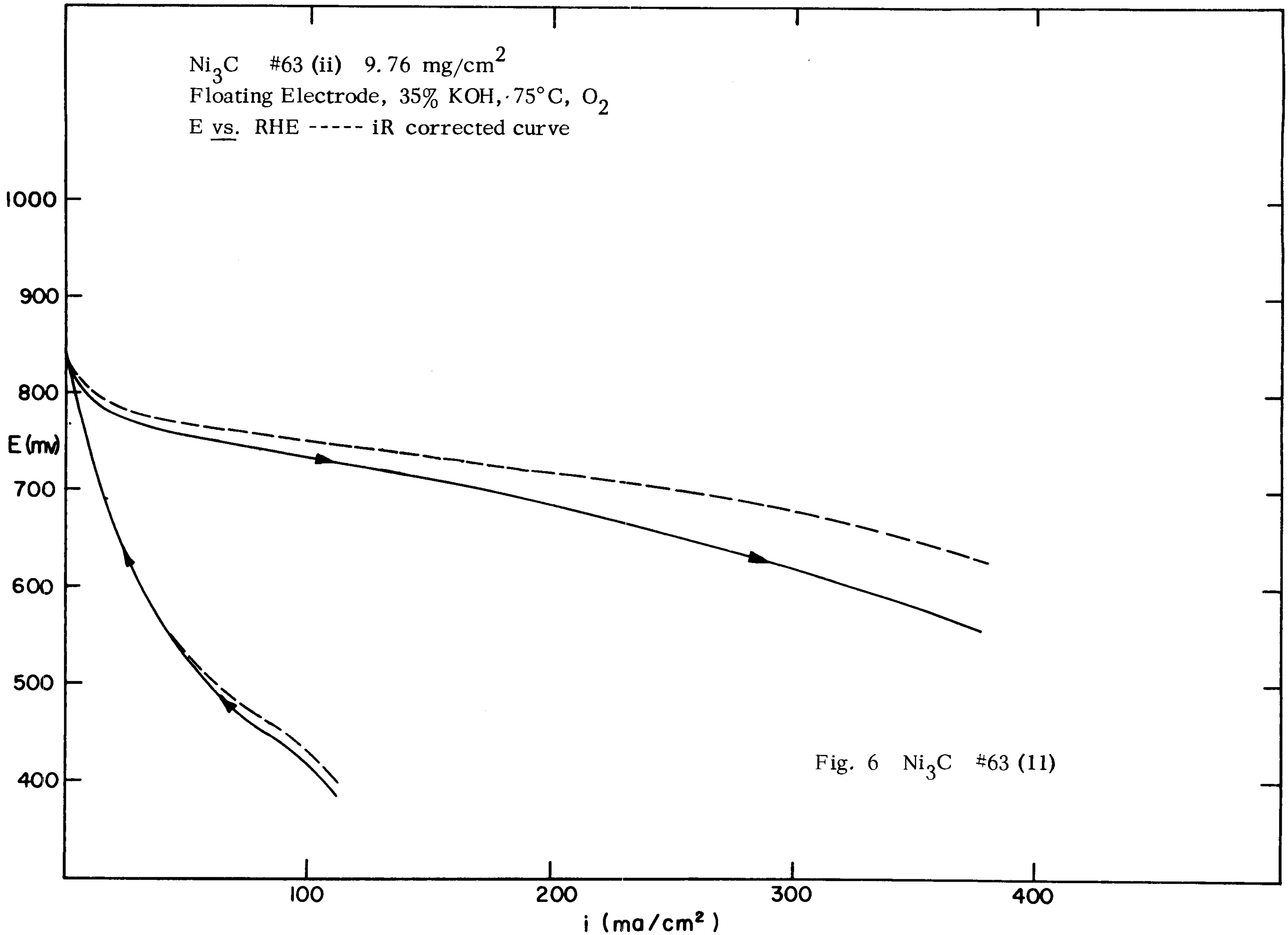

Fig. 6 Ni$_3$C #63 (11)

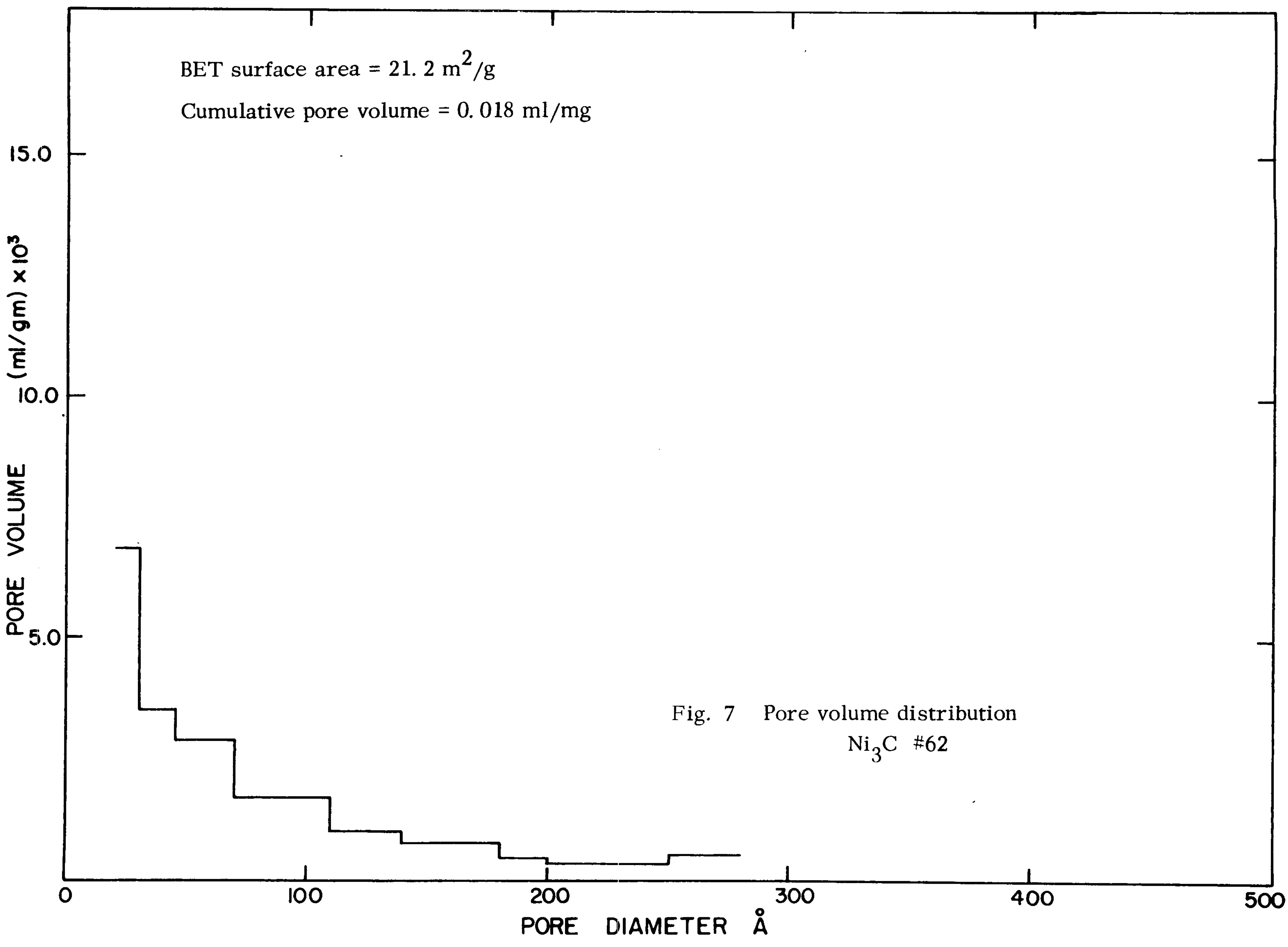

Fig. 7 Pore volume distribution
Ni_3C #62

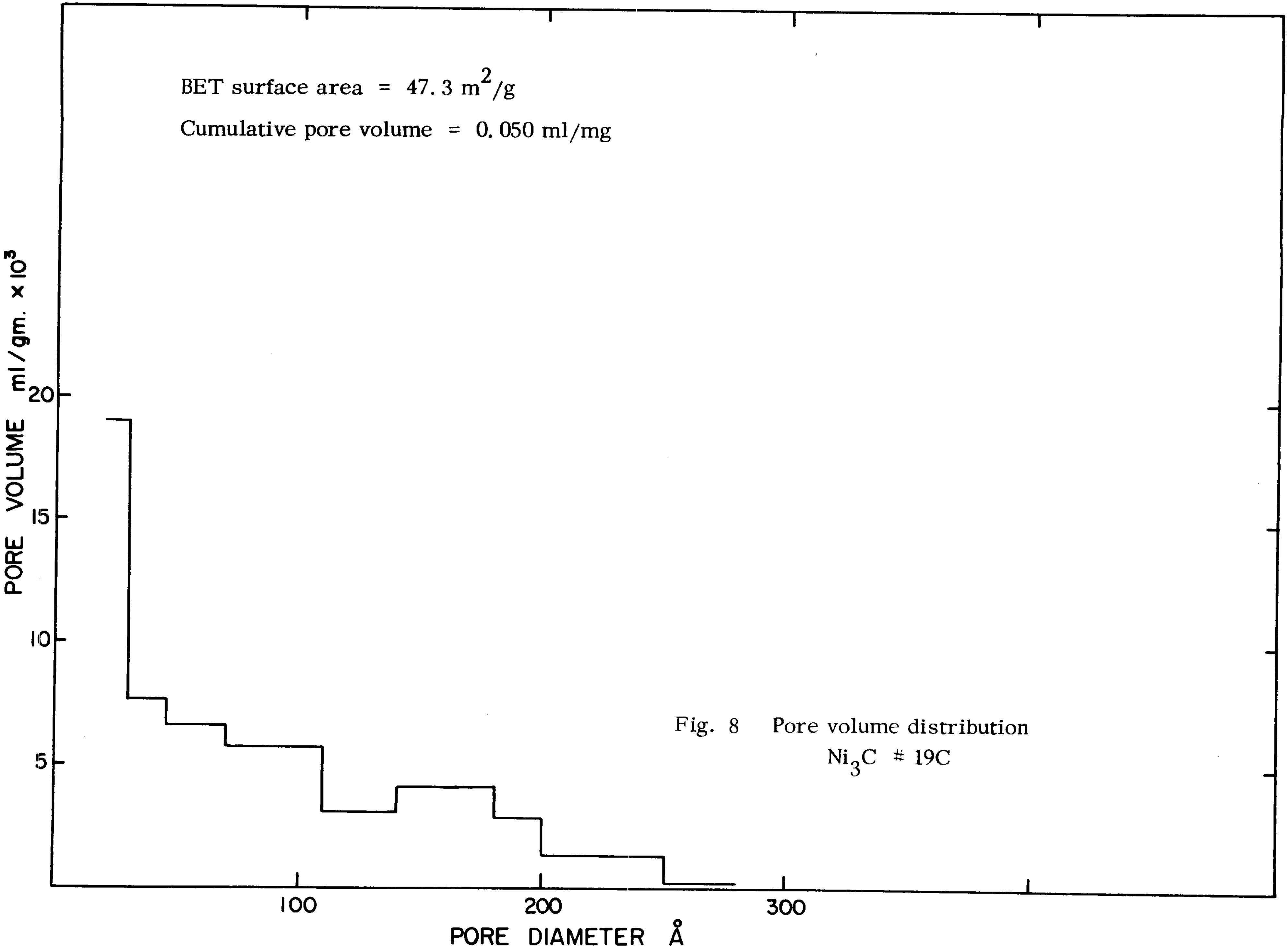

Fig. 8 Pore volume distribution Ni_3C # 19C

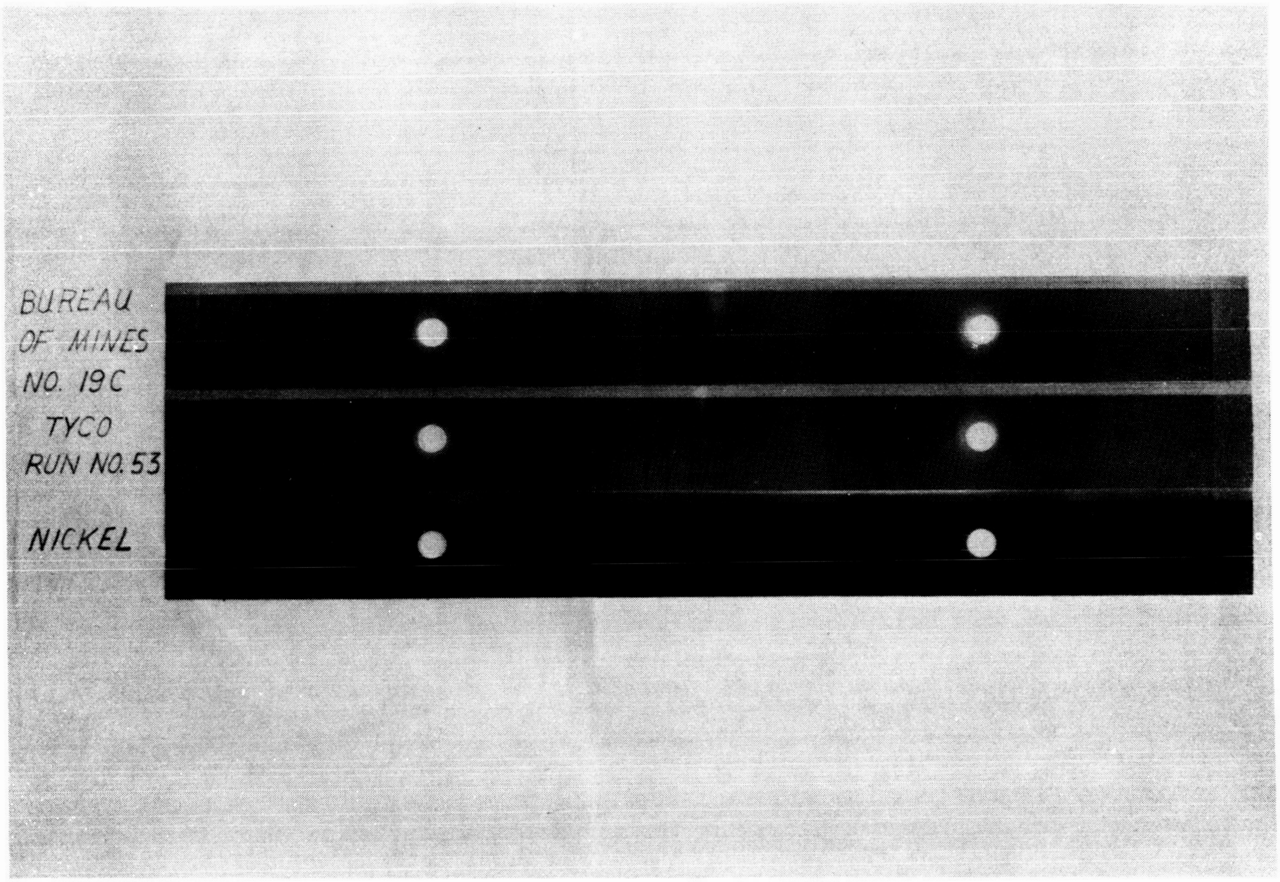

Fig. 9

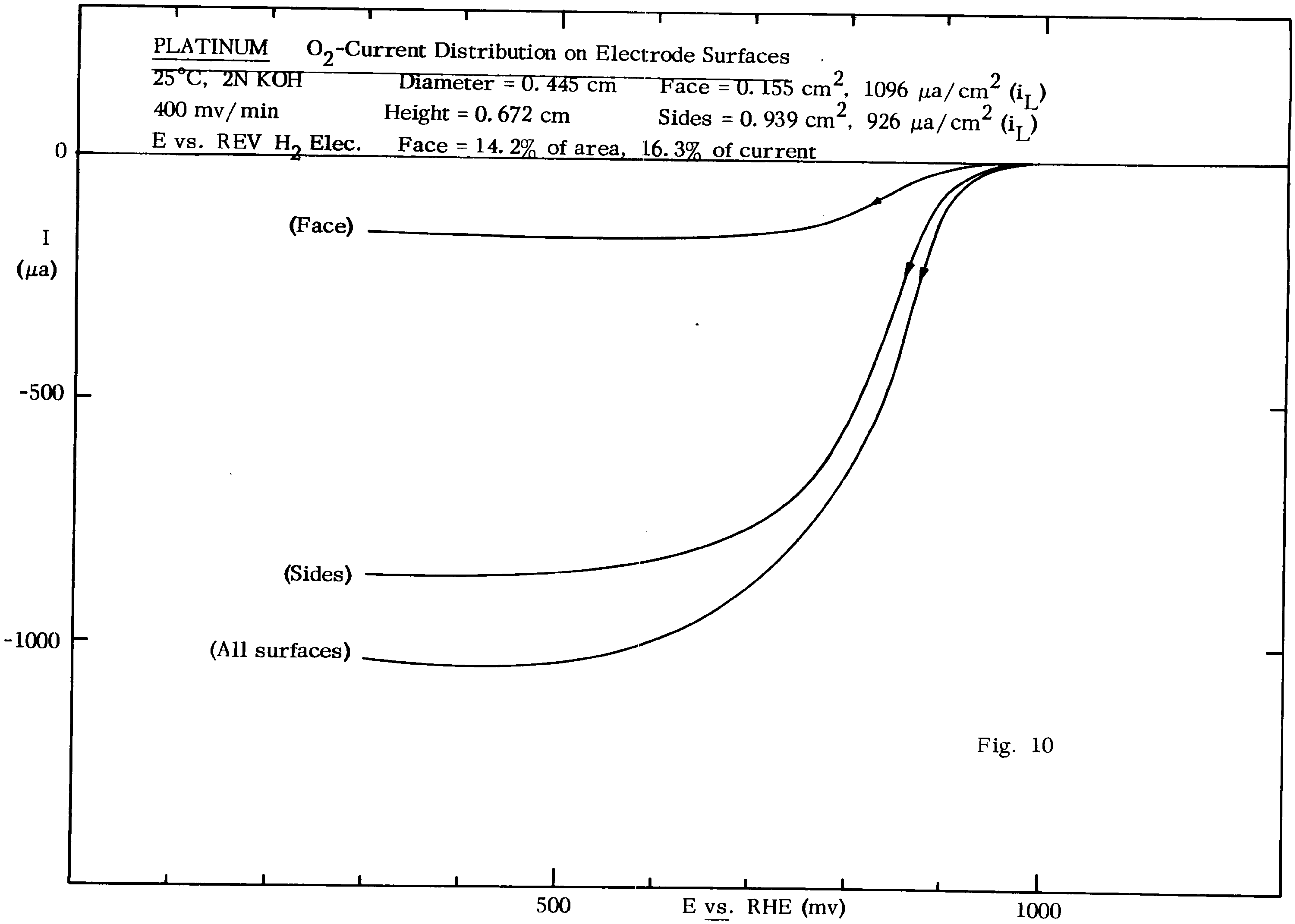

PLATINUM
O_2-Current Distribution on Electrode Surfaces
25°C, 2N KOH
400 mv/min
E vs. REV H_2 Elec.
Diameter = 0.445 cm
Height = 0.672 cm
Face = 14.2% of area, 16.3% of current
Face = 0.155 cm^2, 1096 $\mu a/cm^2$ (i_L)
Sides = 0.939 cm^2, 926 $\mu a/cm^2$ (i_L)
0
-500
-1000
I
(μa)
(Face)
(Sides)
(All surfaces)
500
1000
E vs. RHE (mv)

Fig. 10

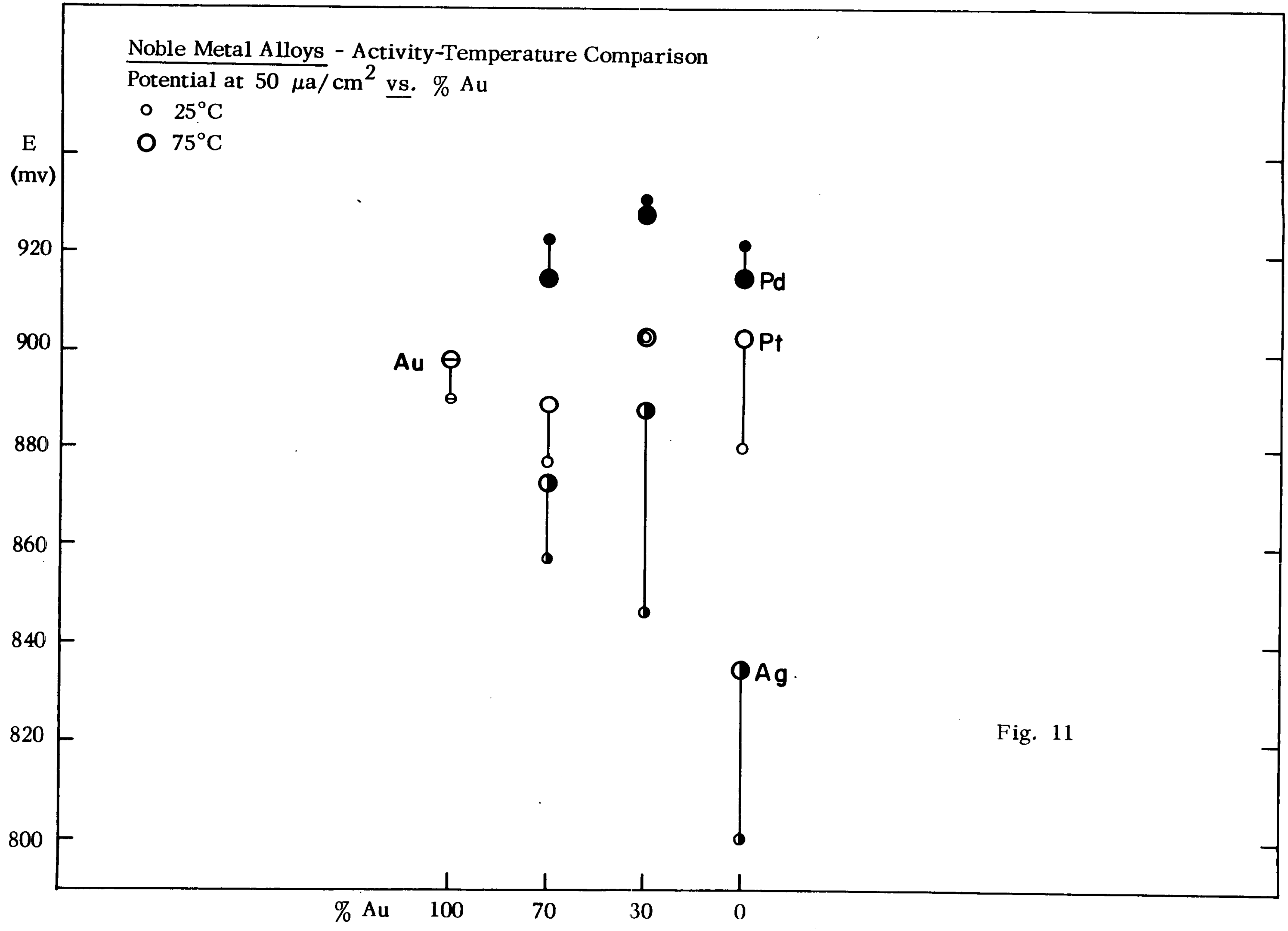
Noble Metal Alloys - Activity-Temperature Comparison
Potential at 50 μa/cm² vs. % Au
25°C
75°C
E (mv)
920
900
880
860
840
820
800
Au
Pd
Pt
Ag
% Au
100
70
30
0

Fig. 11

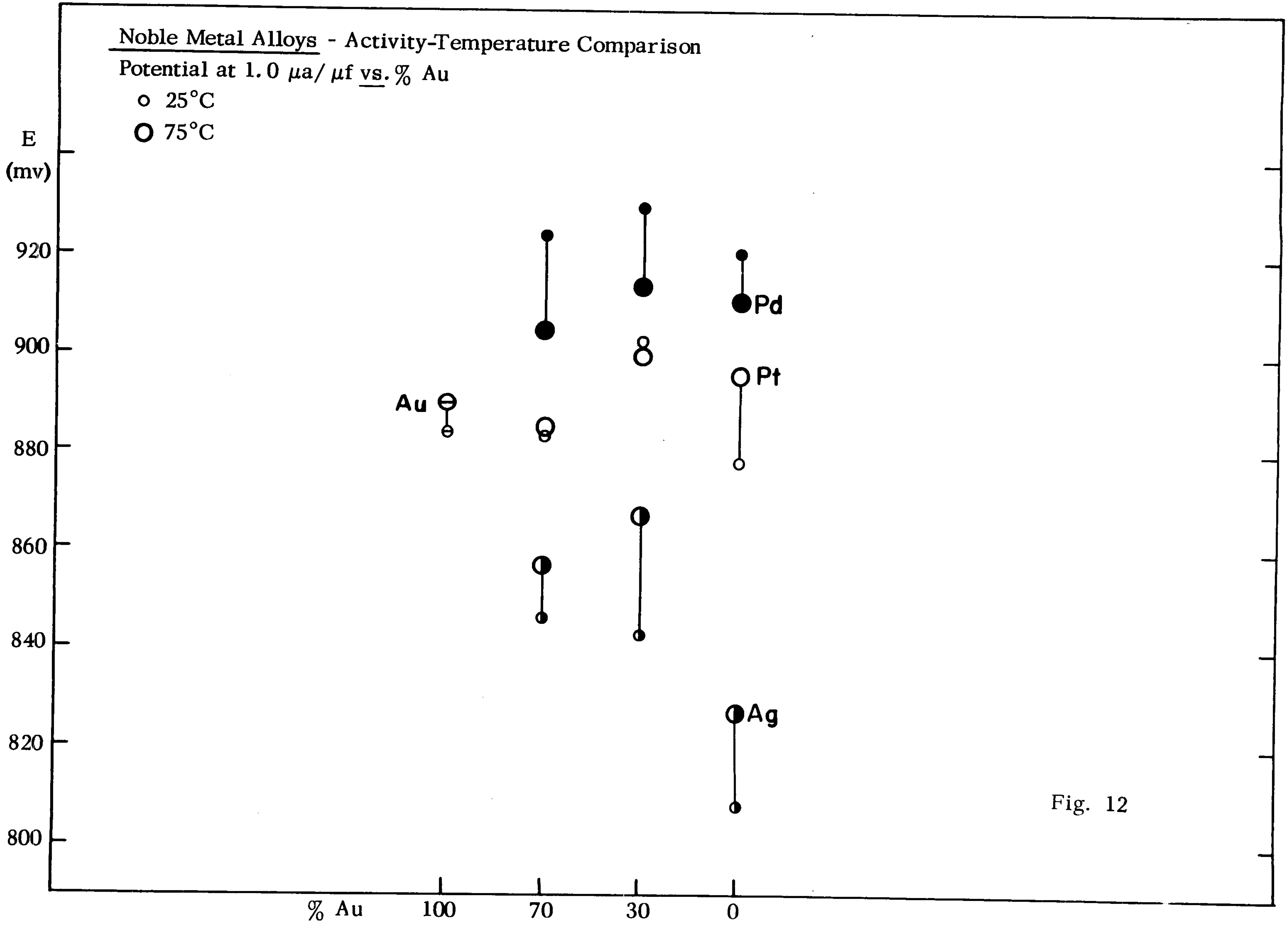
Noble Metal Alloys - Activity-Temperature Comparison
Potential at 1.0 μa/μf vs. % Au
25°C
75°C
E
(mv)
920
900
880
860
840
820
800
% Au
100
70
30
0
Au
Pd
Pt
Ag

Fig. 12

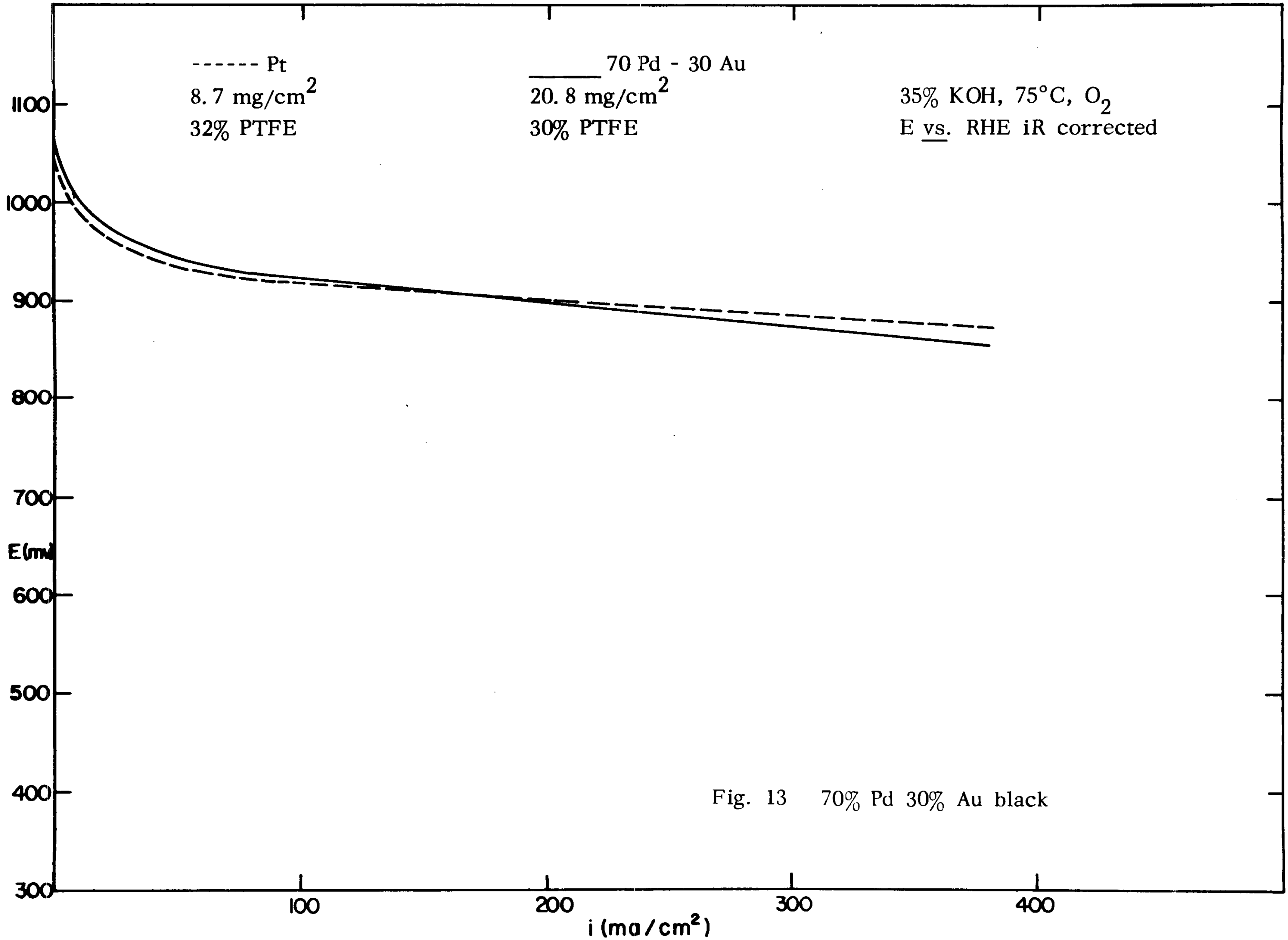

Fig. 13 70% Pd 30% Au black

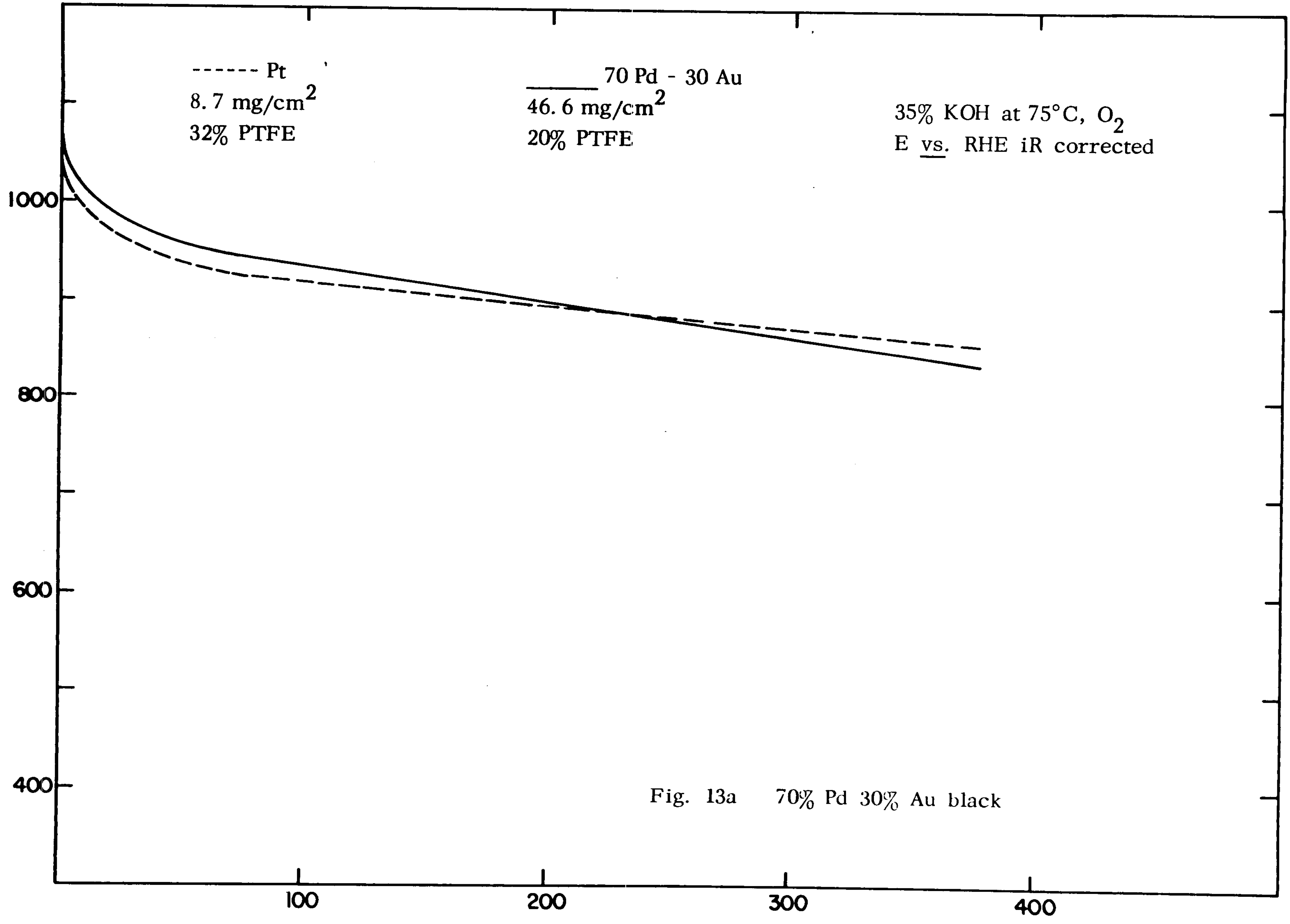

Fig. 13a 70% Pd 30% Au black

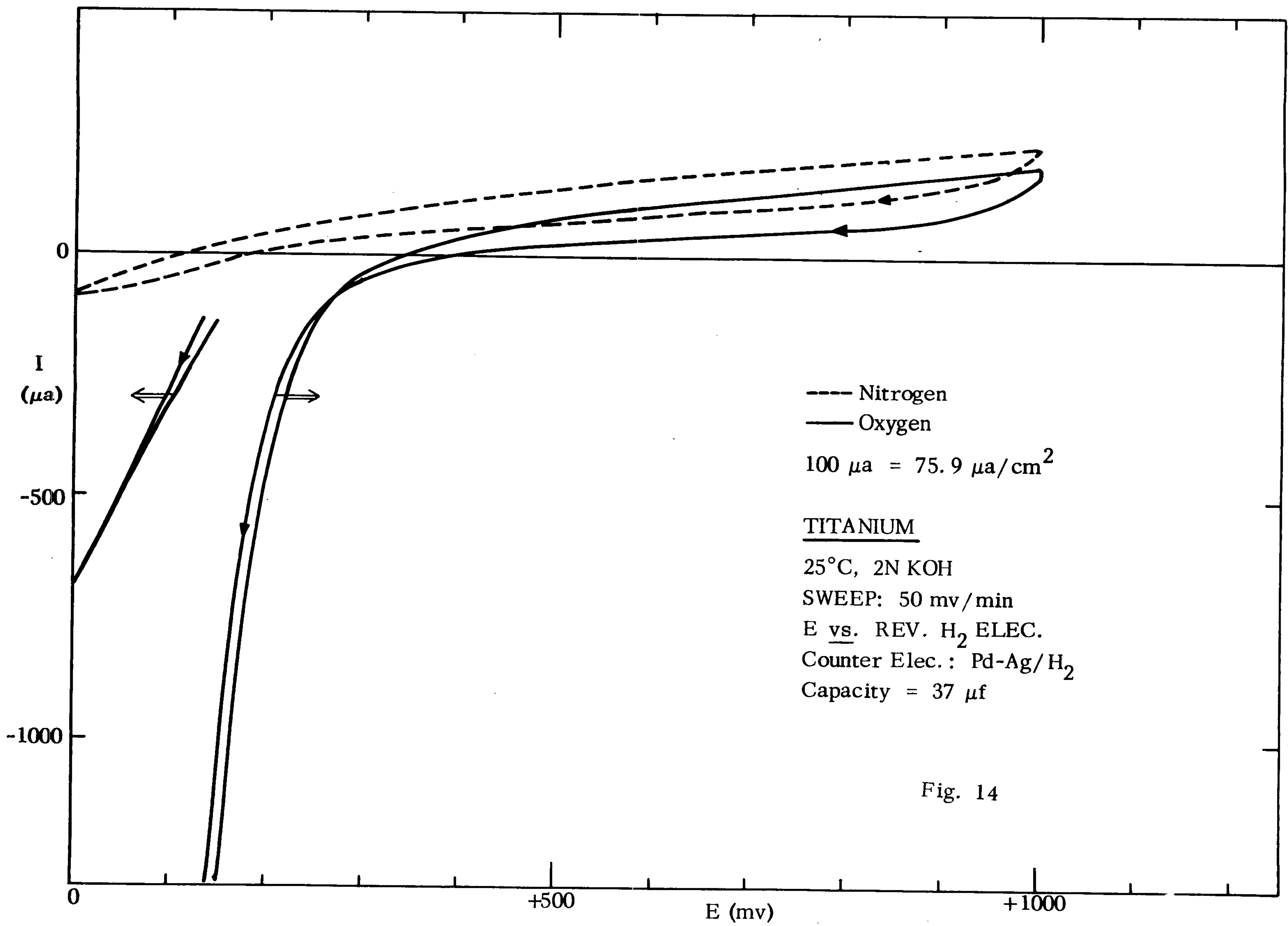

---- Nitrogen
—— Oxygen
100 μa = 75.9 μa/cm²
TITANIUM
25°C, 2N KOH
SWEEP: 50 mv/min
E vs. REV. H₂ ELEC.
Counter Elec.: Pd-Ag/H₂
Capacity = 37 μf
I
(μa)
0
-500
-1000
-5
-1
+500
+1000
E (mv)

Fig. 14

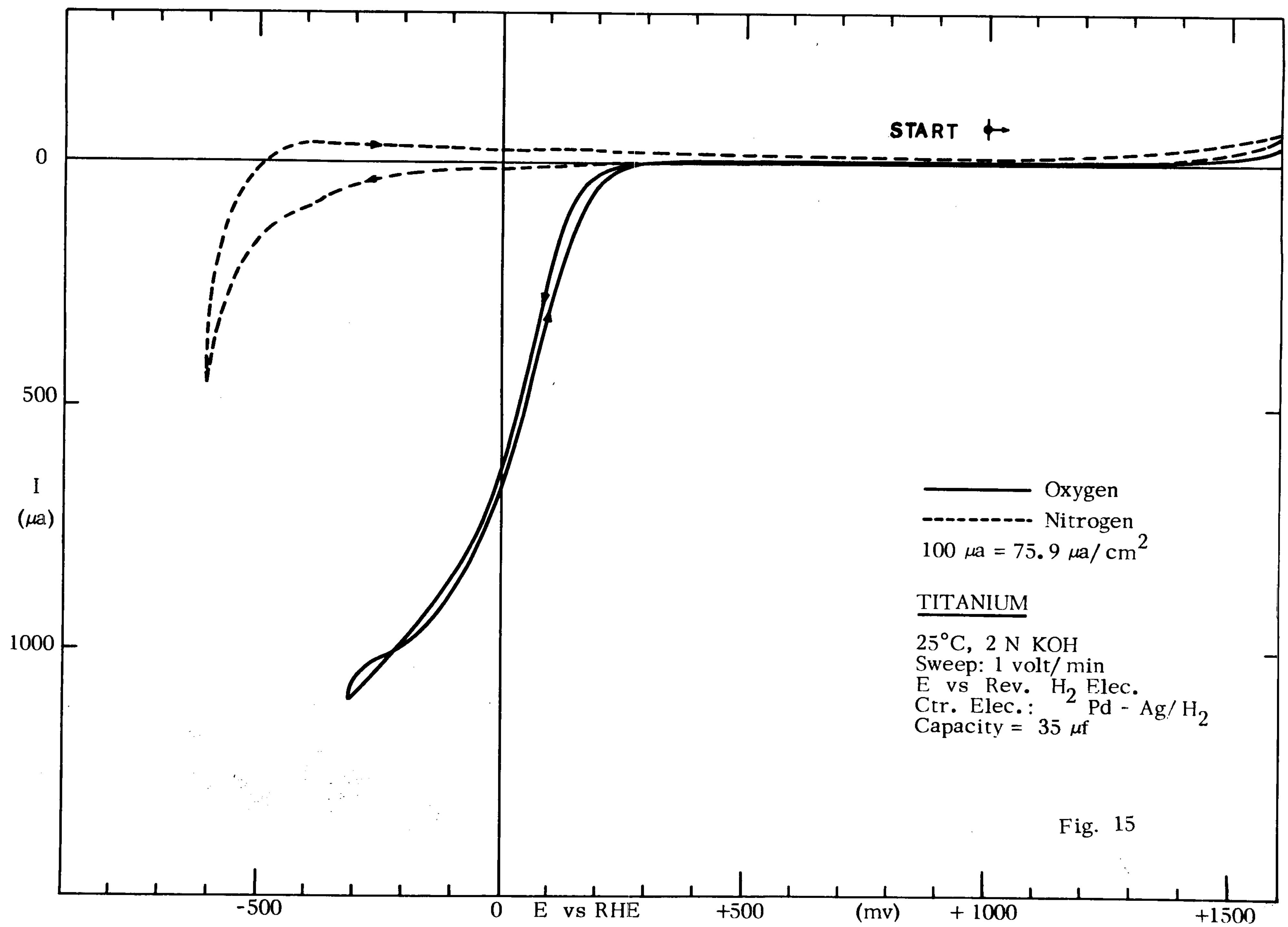
START
0
500
1000
I
(μa)
-500
0
E vs RHE
+500
(mv)
+ 1000
+1500
Oxygen
Nitrogen
100 μa = 75.9 μa/cm²
TITANIUM
25°C, 2 N KOH
Sweep: 1 volt/min
E vs Rev. H₂ Elec.
Ctr. Elec.: Pd - Ag/H₂
Capacity = 35 μf

Fig. 15

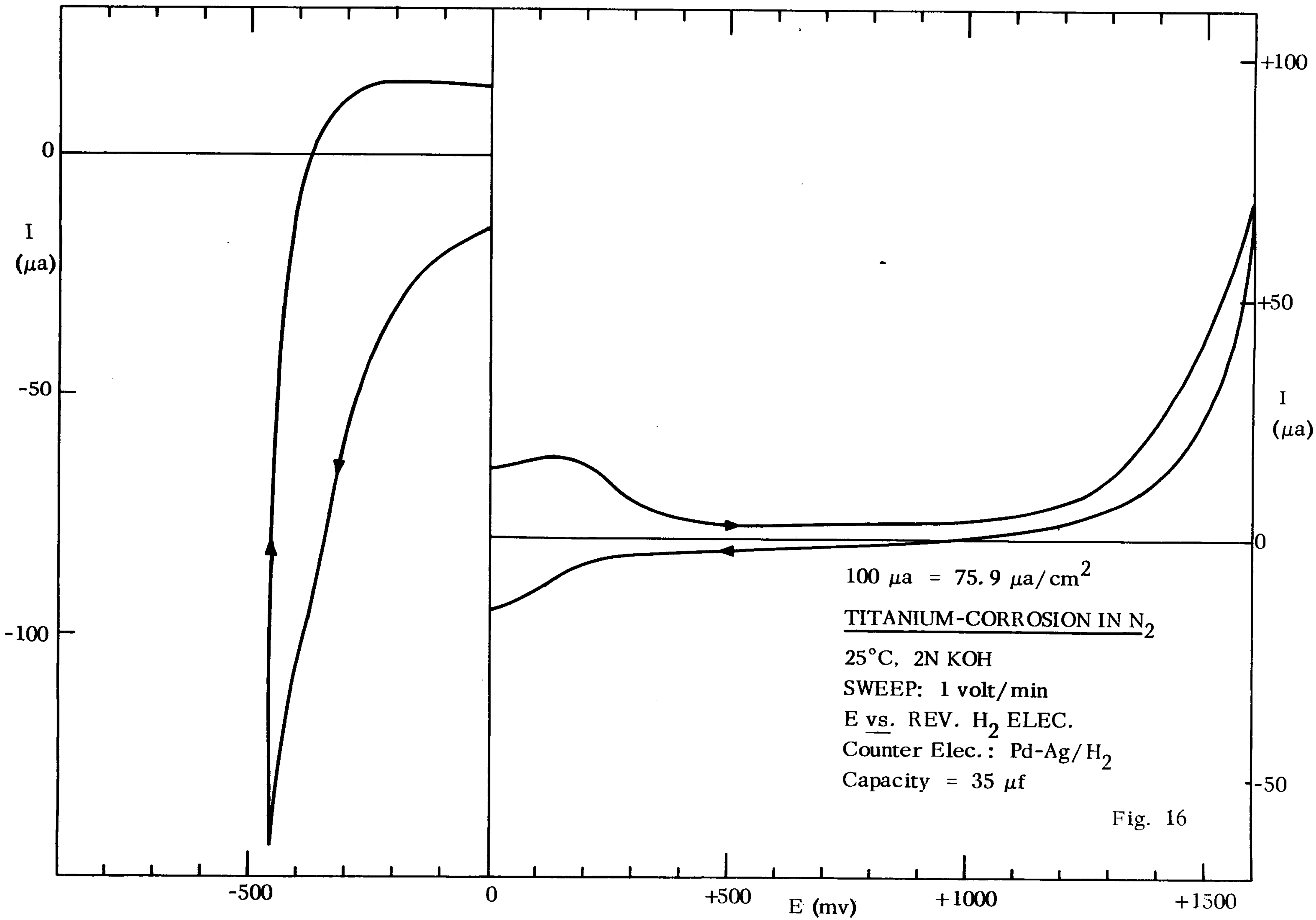
100 μa = 75.9 μa/cm^2
TITANIUM-CORROSION IN N_2
25°C, 2N KOH
SWEEP: 1 volt/min
E vs. REV. H_2 ELEC.
Counter Elec.: Pd-Ag/H_2
Capacity = 35 μf
I (μa)
E (mv)
-500
0
+500
+1000
+1500
-50
-100
+100
+50
Fig. 16

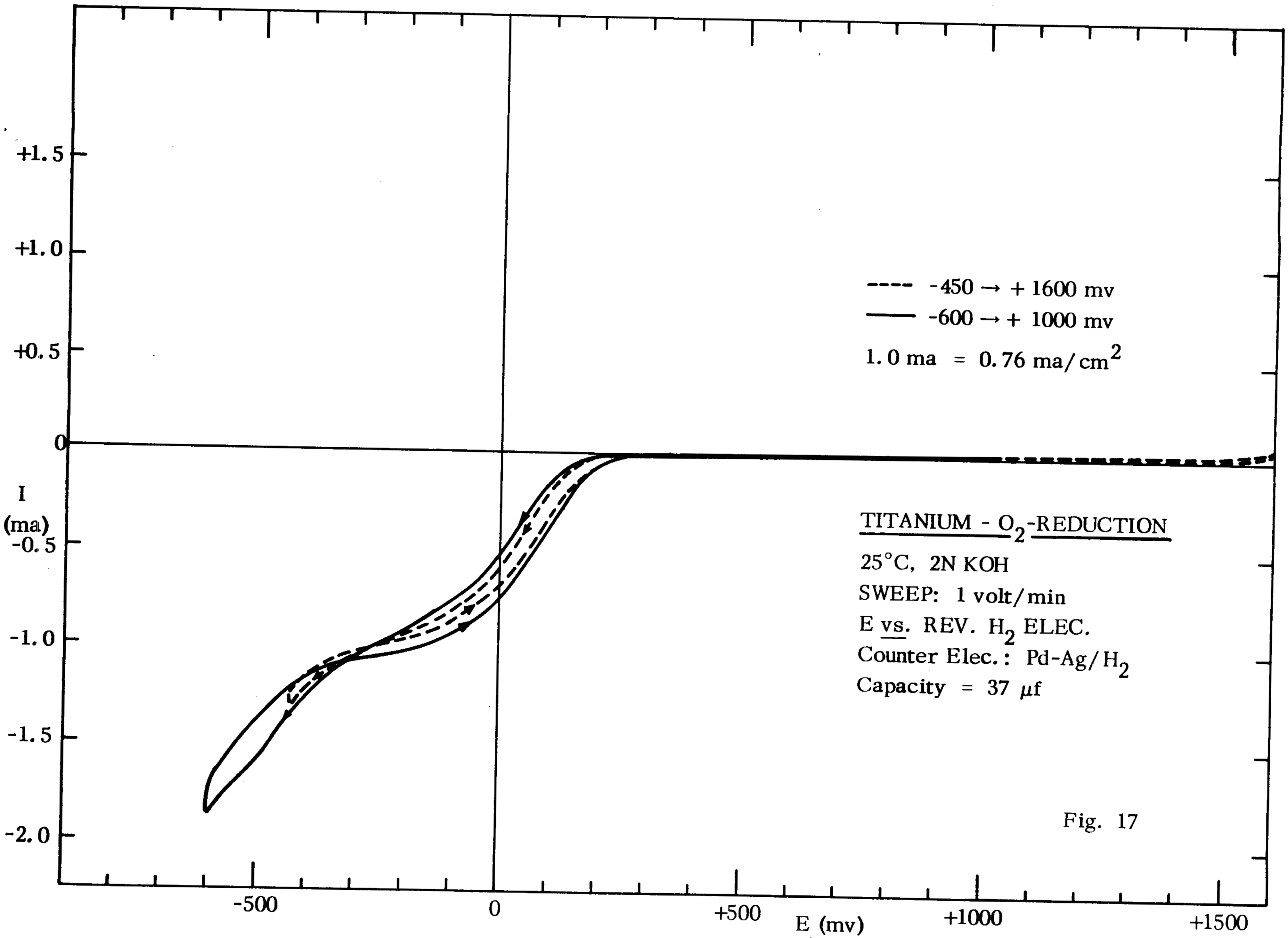

+1.5
+1.0
+0.5
0
I
(ma)
-0.5
-1.0
-1.5
-2.0
-500
0
+500
+1000
+1500
E (mv)
---- -450 → + 1600 mv
—— -600 → + 1000 mv
1.0 ma = 0.76 ma/cm²
TITANIUM - O₂-REDUCTION
25°C, 2N KOH
SWEEP: 1 volt/min
E vs. REV. H₂ ELEC.
Counter Elec.: Pd-Ag/H₂
Capacity = 37 μf

Fig. 17

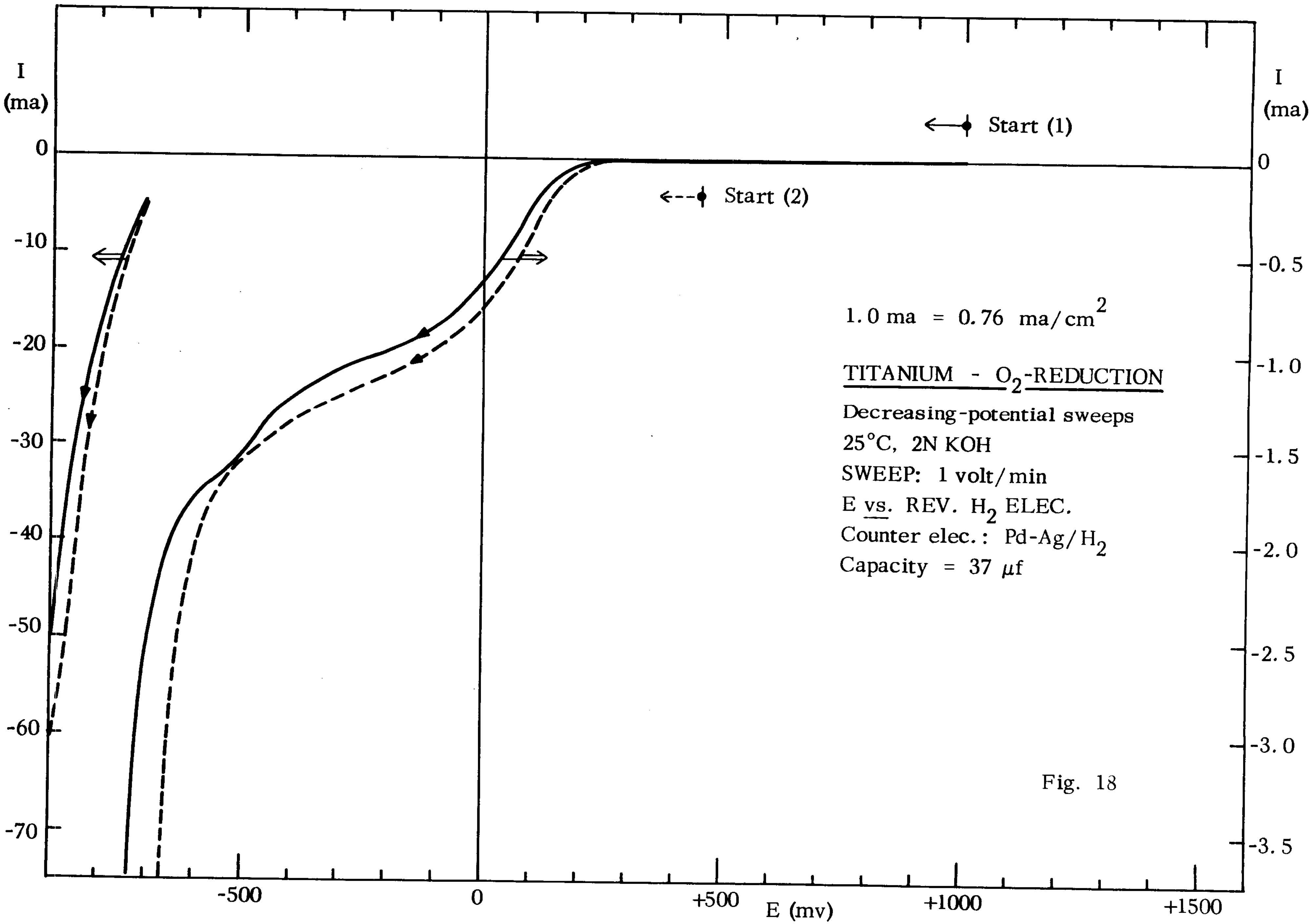

I (ma)
0
-10
-20
-30
-40
-50
-60
-70
Start (1)
Start (2)
1.0 ma = 0.76 ma/cm^2
TITANIUM - O_2-REDUCTION
Decreasing-potential sweeps
25°C, 2N KOH
SWEEP: 1 volt/min
E vs. REV. H_2 ELEC.
Counter elec.: Pd-Ag/H_2
Capacity = 37 μf
I (ma)
0
-0.5
-1.0
-1.5
-2.0
-2.5
-3.0
-3.5
-500
0
+500
+1000
+1500
E (mv)

Fig. 18

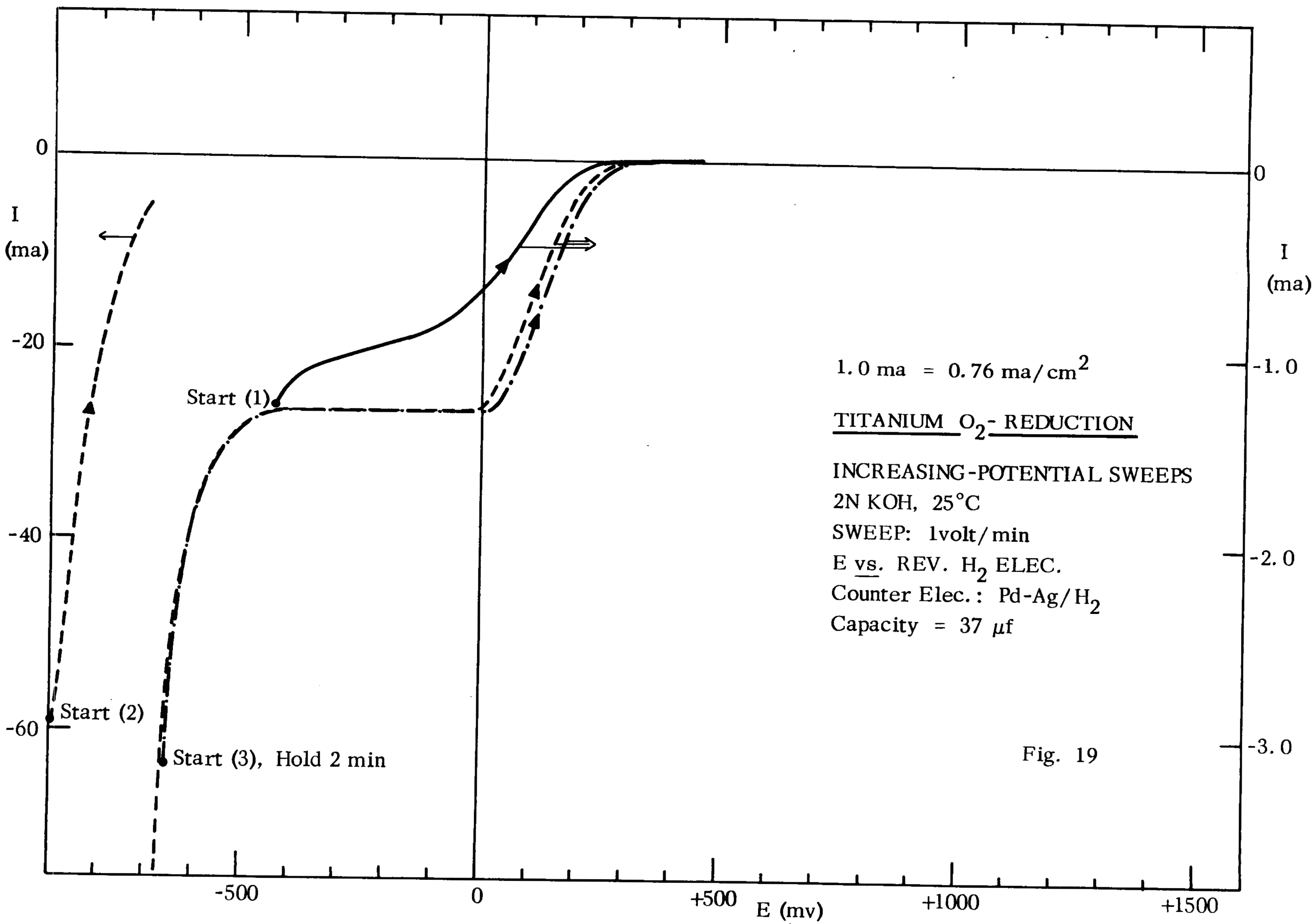

0
I
(ma)
-20
-40
-60
0
I
(ma)
-1.0
-2.0
-3.0
-500
0
+500
E (mv)
+1000
+1500
Start (1)
Start (2)
Start (3), Hold 2 min
1.0 ma = 0.76 ma/cm^2
TITANIUM O_2- REDUCTION
INCREASING-POTENTIAL SWEEPS
2N KOH, 25°C
SWEEP: 1volt/min
E vs. REV. H_2 ELEC.
Counter Elec.: Pd-Ag/H_2
Capacity = 37 μf

Fig. 19

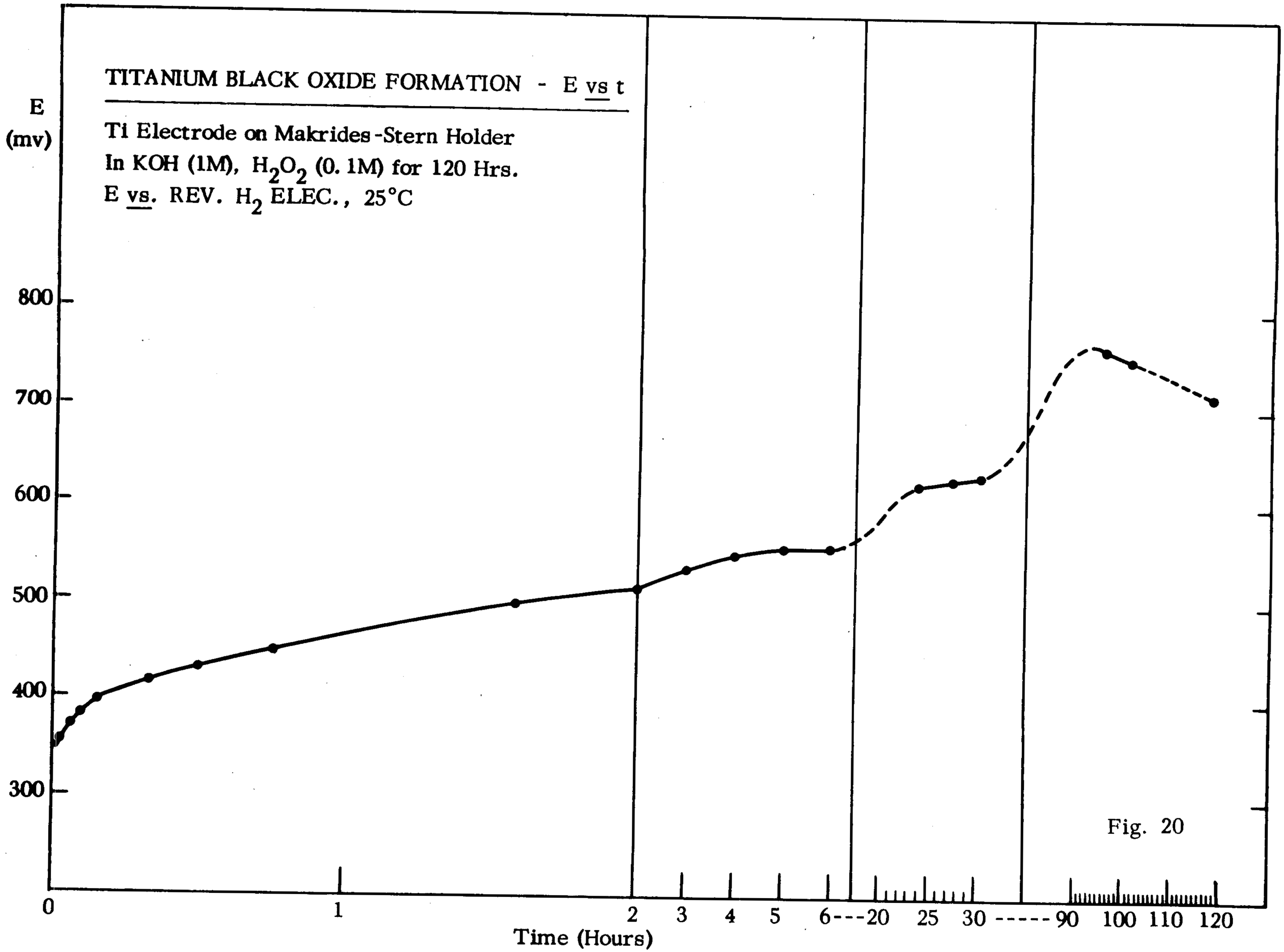

TITANIUM BLACK OXIDE FORMATION - E vs t
Ti Electrode on Makrides-Stern Holder
In KOH (1M), H2O2 (0.1M) for 120 Hrs.
E vs. REV. H2 ELEC., 25°C
E
(mv)
800
700
600
500
400
300
0
1
2
3
4
5
6---20
25
30 -----90
100
110
120
Time (Hours)

Fig. 20

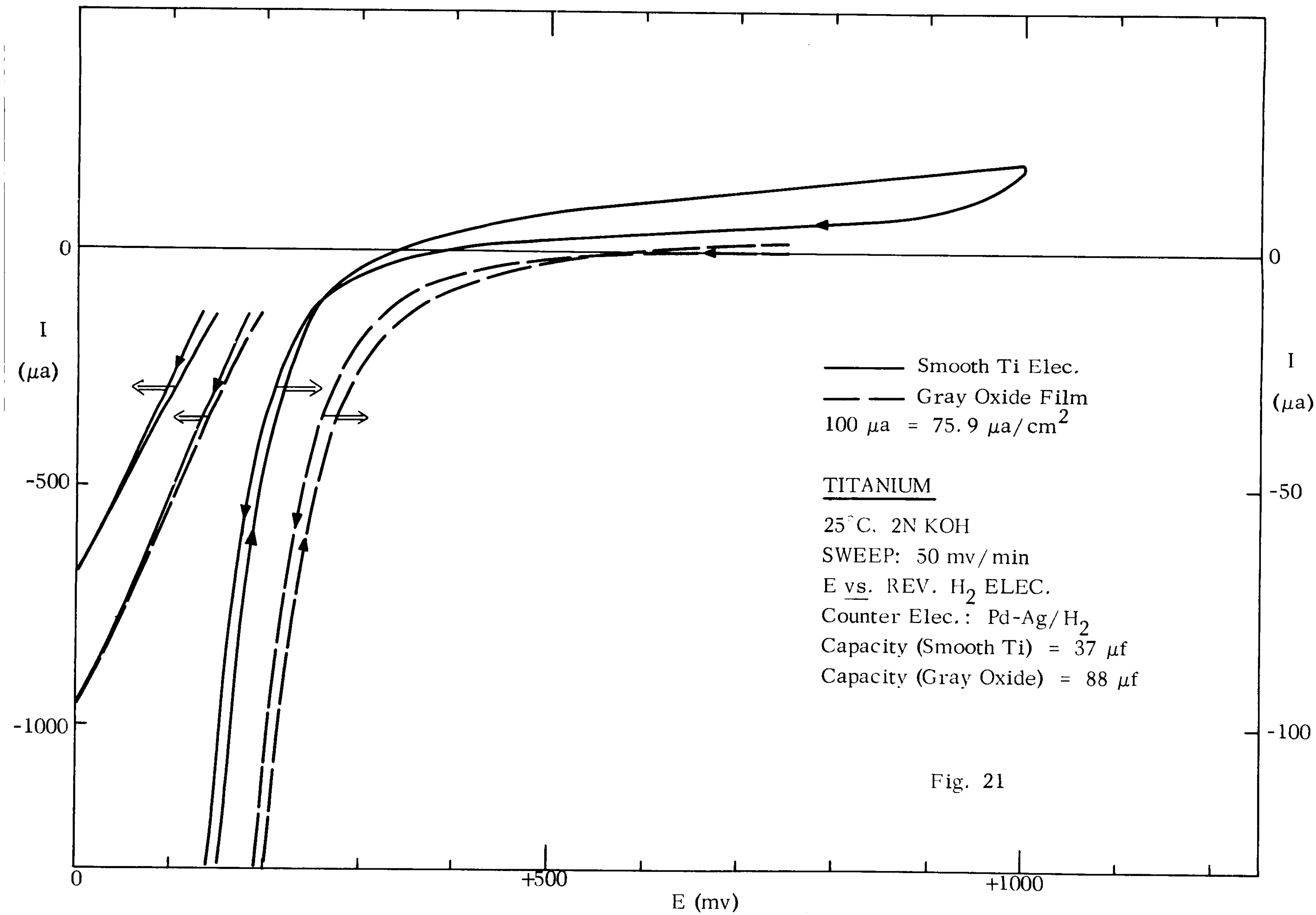

I
(μa)
0
-500
-1000
0
-50
-100
0
+500
+1000
E (mv)
Smooth Ti Elec.
Gray Oxide Film
100 μa = 75.9 μa/cm²
TITANIUM
25°C. 2N KOH
SWEEP: 50 mv/min
E vs. REV. H₂ ELEC.
Counter Elec.: Pd-Ag/H₂
Capacity (Smooth Ti) = 37 μf
Capacity (Gray Oxide) = 88 μf

Fig. 21

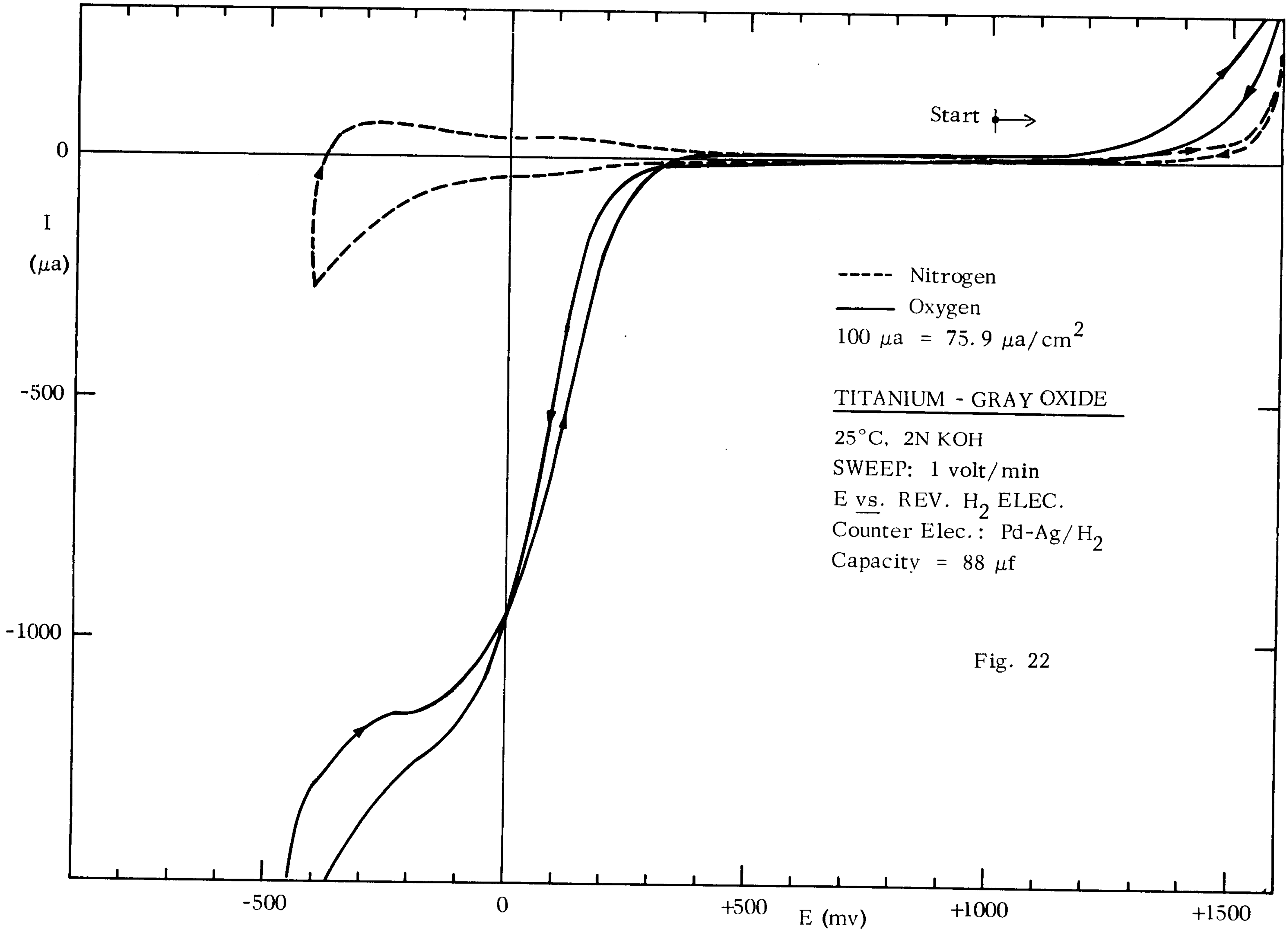

Start
0
I
(μa)
-500
-1000
Nitrogen
Oxygen
100 μa = 75. 9 μa/cm2
TITANIUM - GRAY OXIDE
25°C, 2N KOH
SWEEP: 1 volt/min
E vs. REV. H2 ELEC.
Counter Elec.: Pd-Ag/H2
Capacity = 88 μf
-500
0
+500
E (mv)
+1000
+1500

Fig. 22

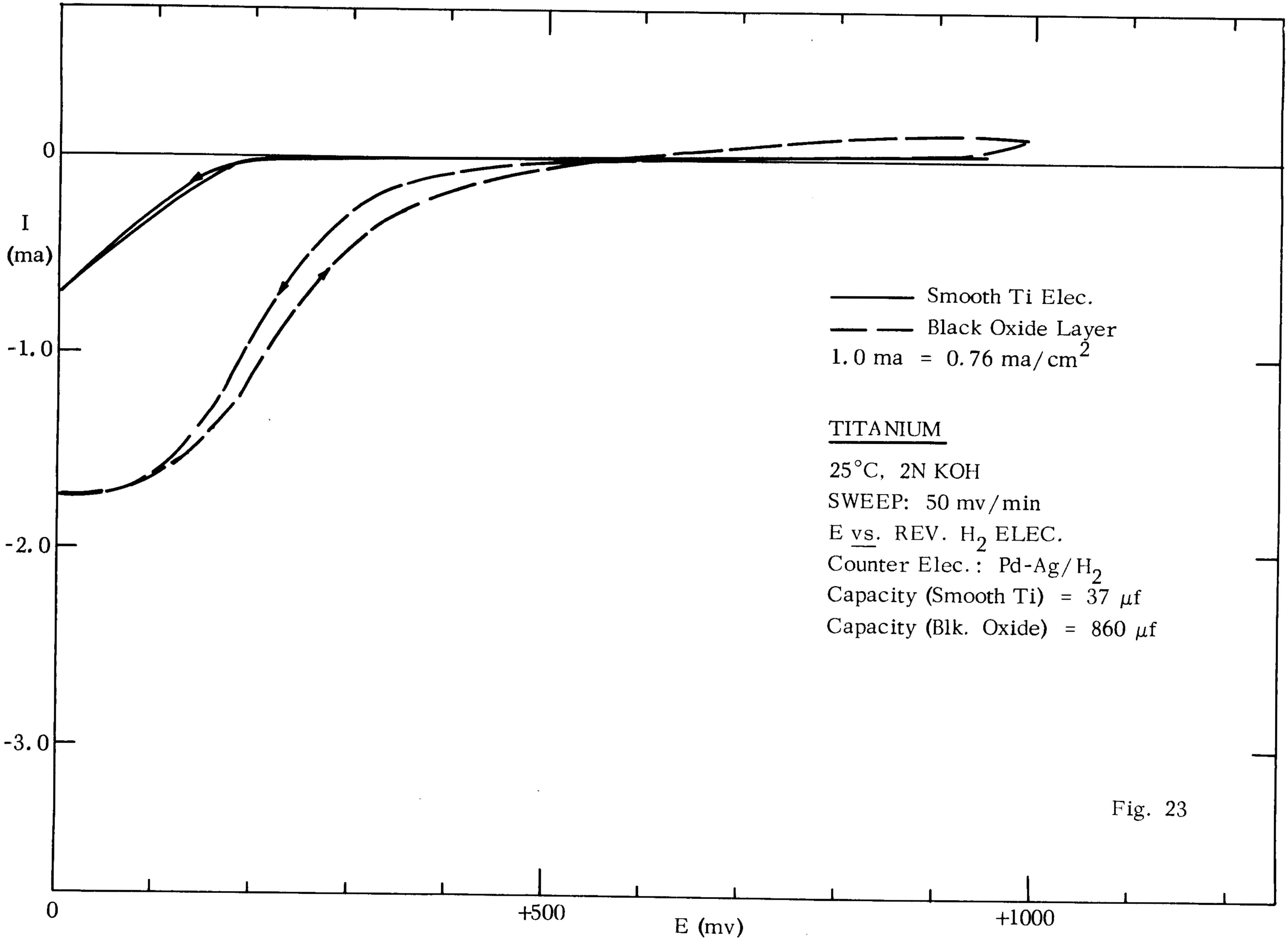

0
-1.0
-2.0
-3.0
I
(ma)
0
+500
+1000
E (mv)
Smooth Ti Elec.
Black Oxide Layer
1.0 ma = 0.76 ma/cm²
TITANIUM
25°C, 2N KOH
SWEEP: 50 mv/min
E vs. REV. H₂ ELEC.
Counter Elec.: Pd-Ag/H₂
Capacity (Smooth Ti) = 37 μf
Capacity (Blk. Oxide) = 860 μf

Fig. 23

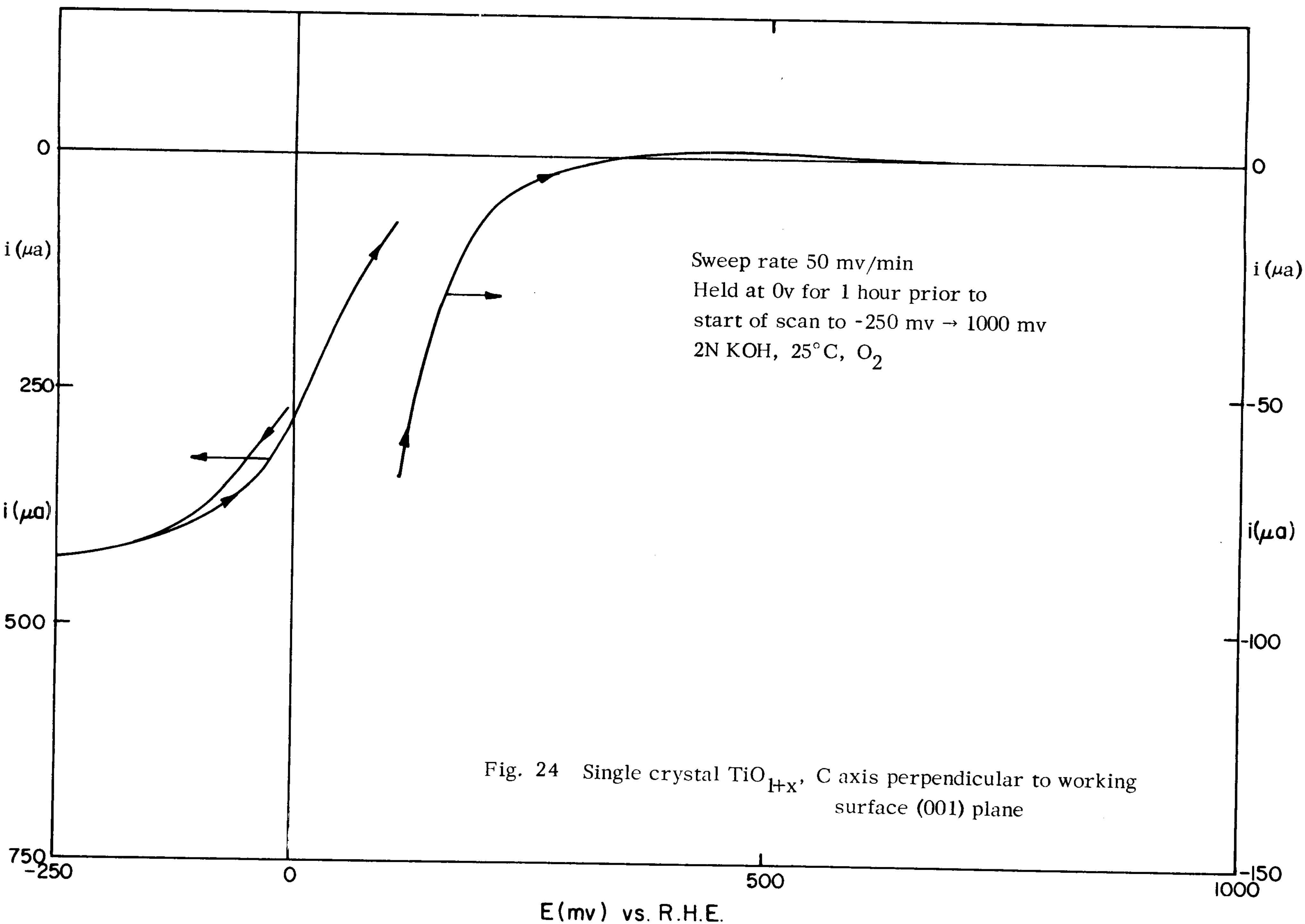

Fig. 24 Single crystal TiO_{1+x}, C axis perpendicular to working surface (001) plane

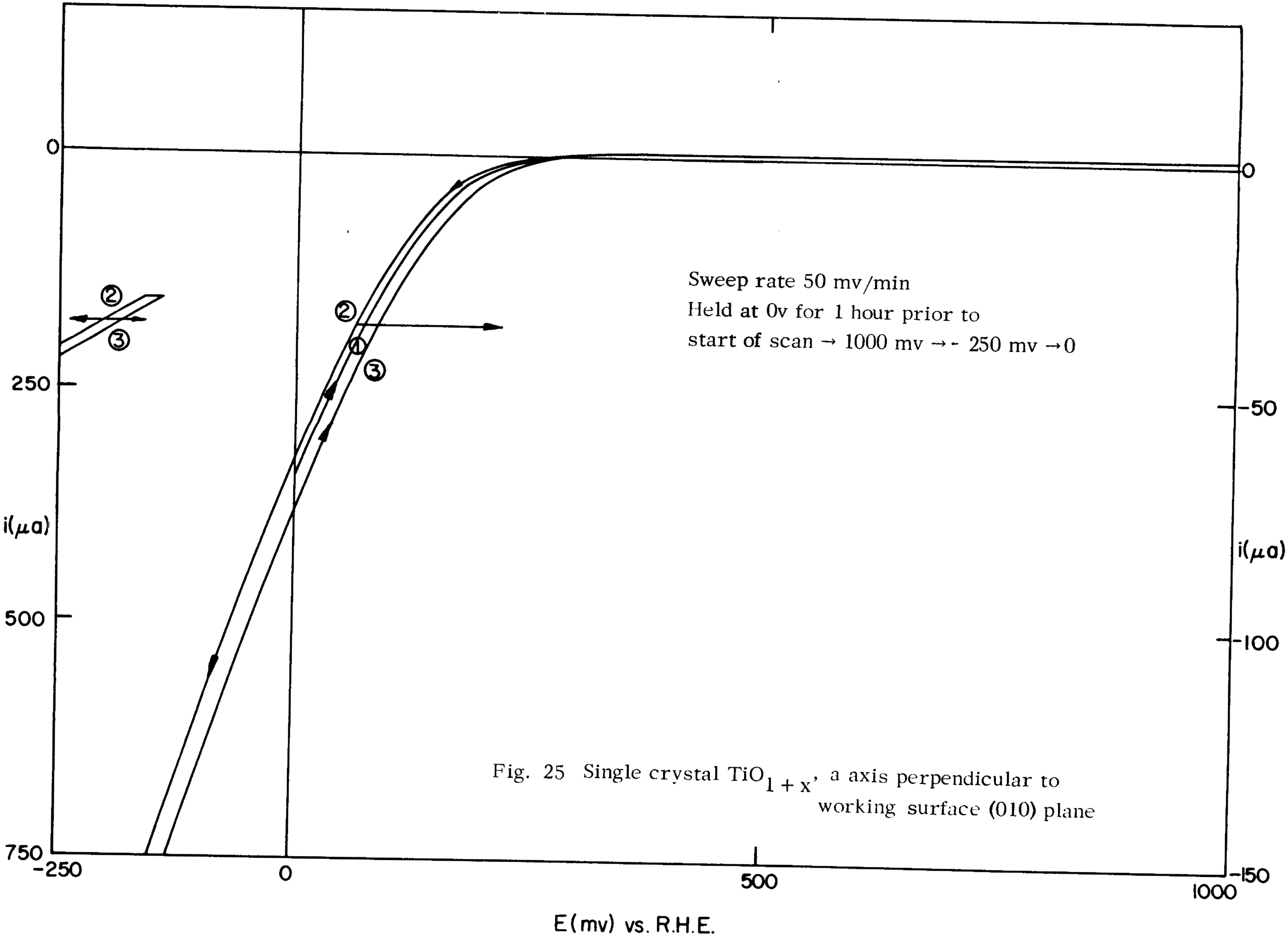

Fig. 25 Single crystal TiO_{1+x}, a axis perpendicular to working surface (010) plane

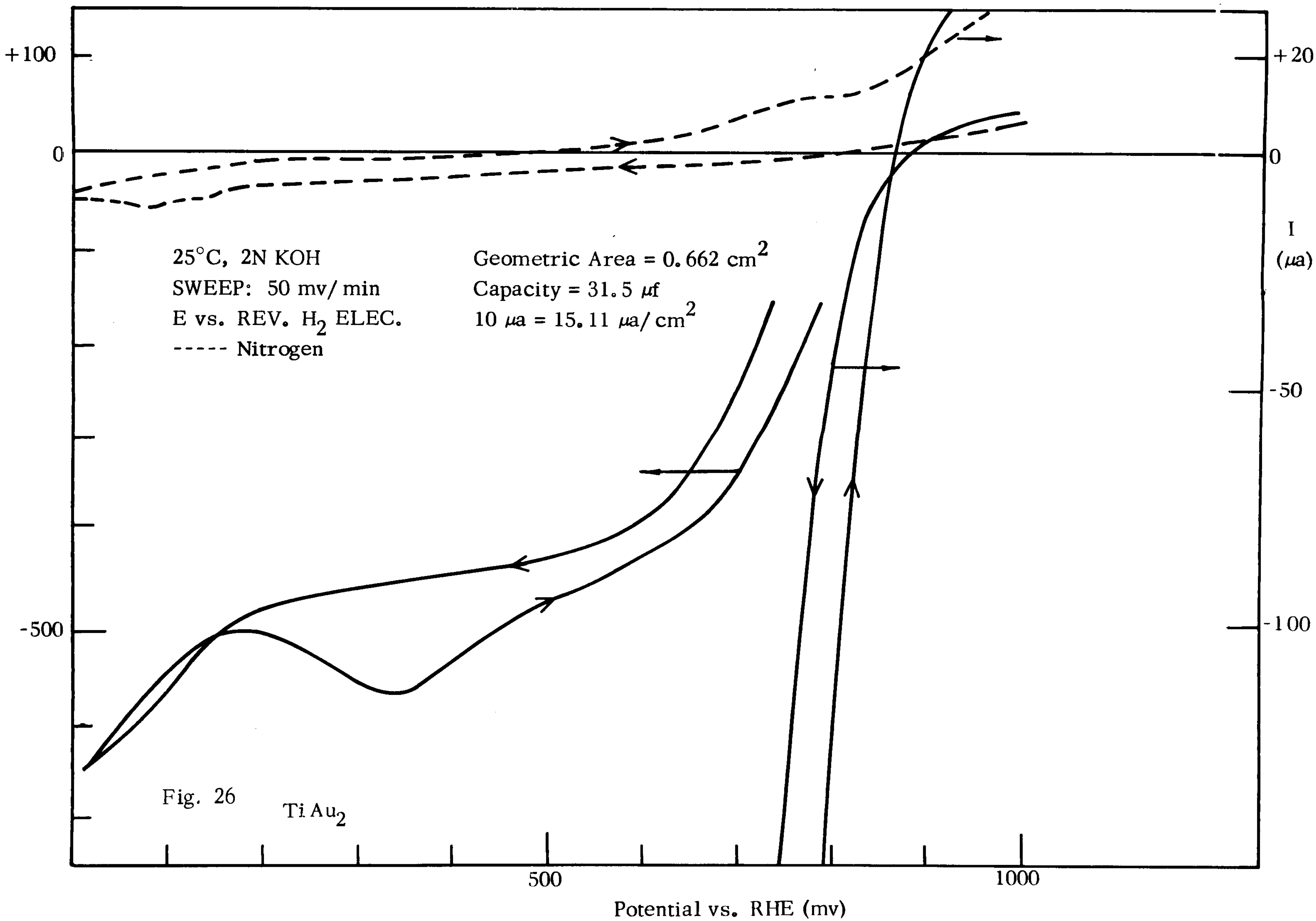

+100
0
-500
+20
0
I
(μa)
-50
-100
25°C, 2N KOH
SWEEP: 50 mv/min
E vs. REV. H2 ELEC.
----- Nitrogen
Geometric Area = 0.662 cm2
Capacity = 31.5 μf
10 μa = 15.11 μa/cm2
500
1000
Potential vs. RHE (mv)

Fig. 26 Ti Au_2

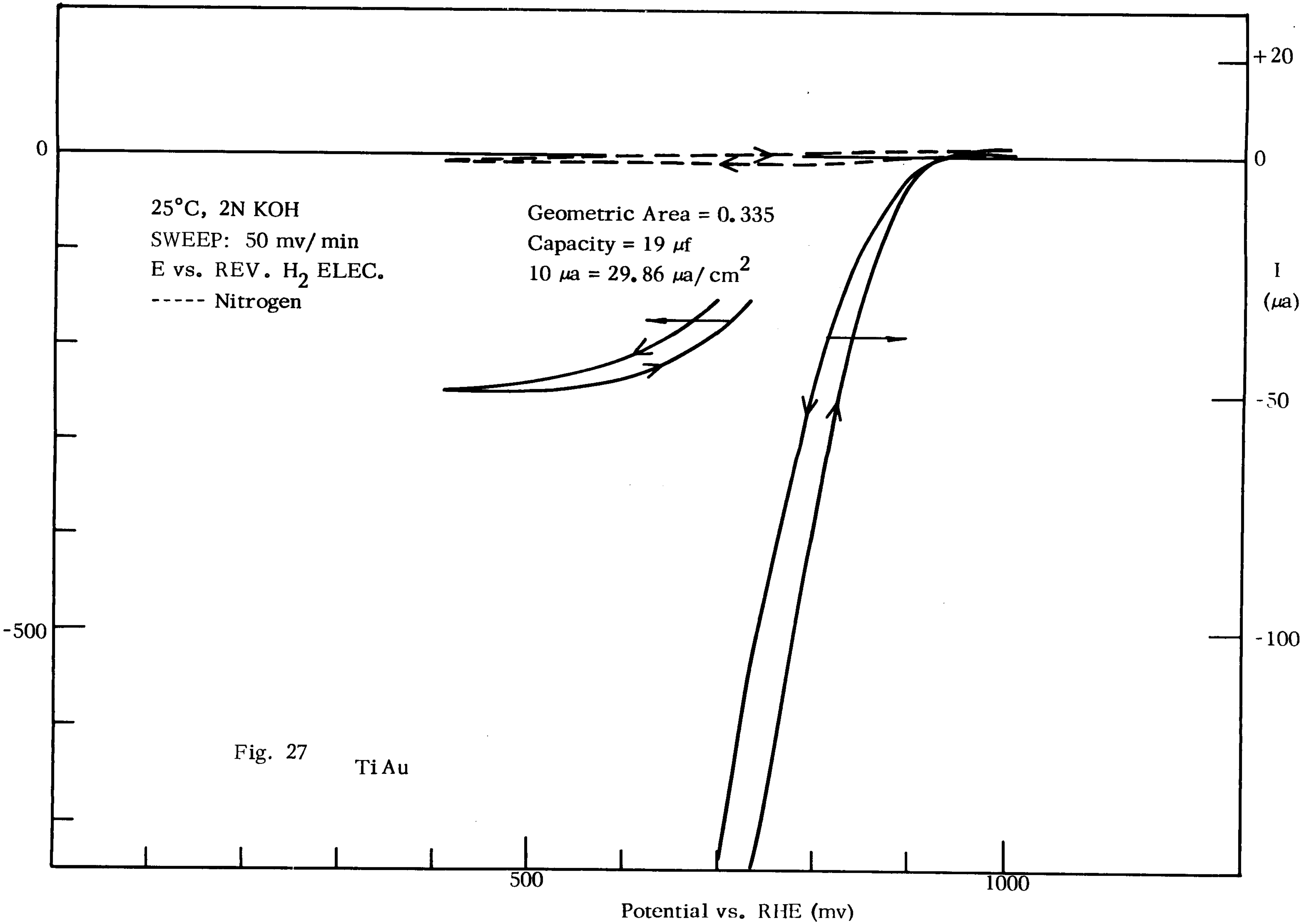
0
-500
+20
0
I
(μa)
-50
-100
500
1000
Potential vs. RHE (mv)
25°C, 2N KOH
SWEEP: 50 mv/ min
E vs. REV. H2 ELEC.
----- Nitrogen
Geometric Area = 0.335
Capacity = 19 μf
10 μa = 29.86 μa/ cm2
Ti Au
Fig. 27

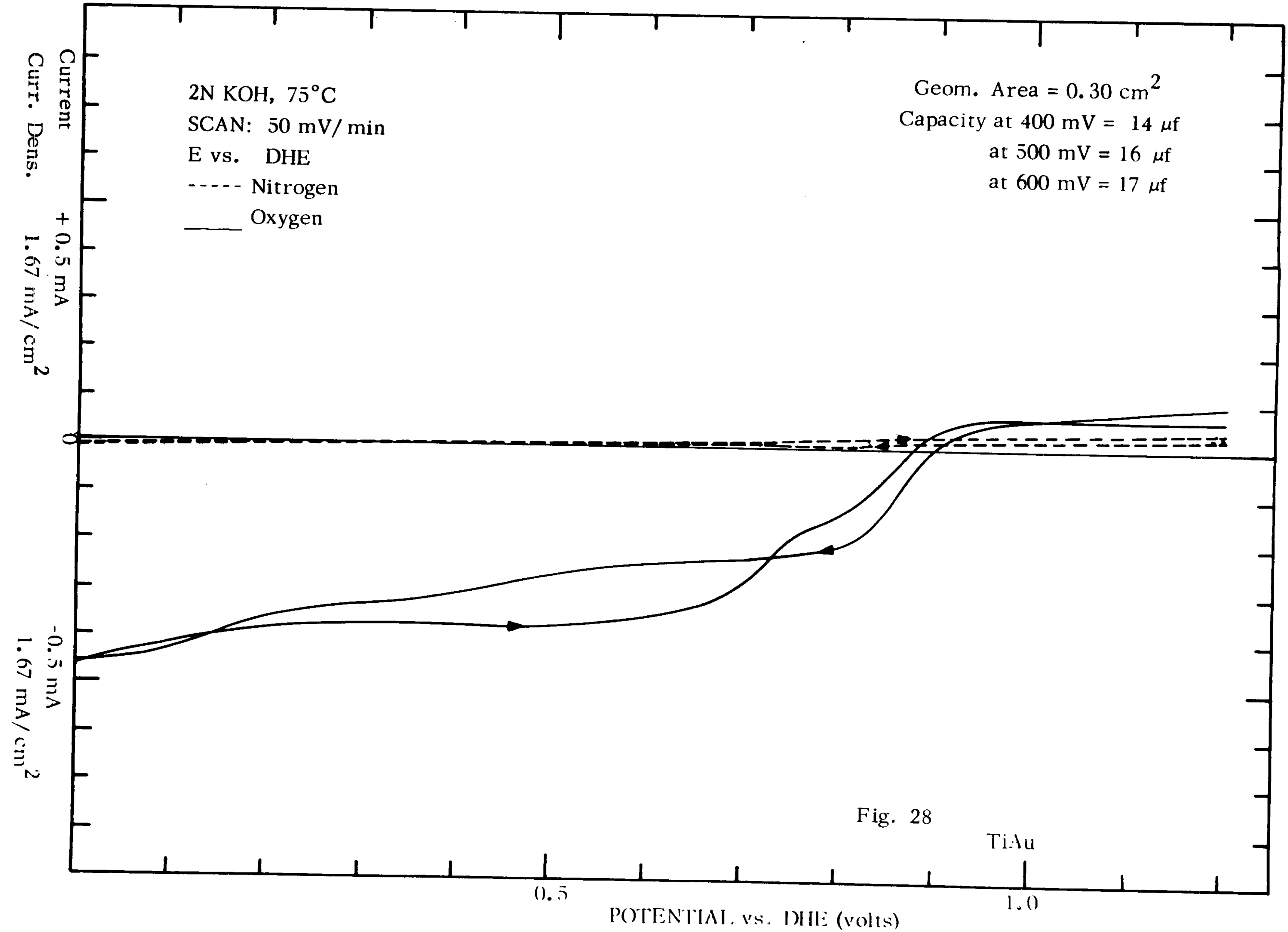
Current
Curr. Dens.
+ 0.5 mA
1.67 mA/cm²
0
-0.5 mA
1.67 mA/cm²
2N KOH, 75°C
SCAN: 50 mV/min
E vs. DHE
----- Nitrogen
_____ Oxygen
Geom. Area = 0.30 cm²
Capacity at 400 mV = 14 μf
at 500 mV = 16 μf
at 600 mV = 17 μf
0.5
1.0
POTENTIAL vs. DHE (volts)

Fig. 28
TiAu

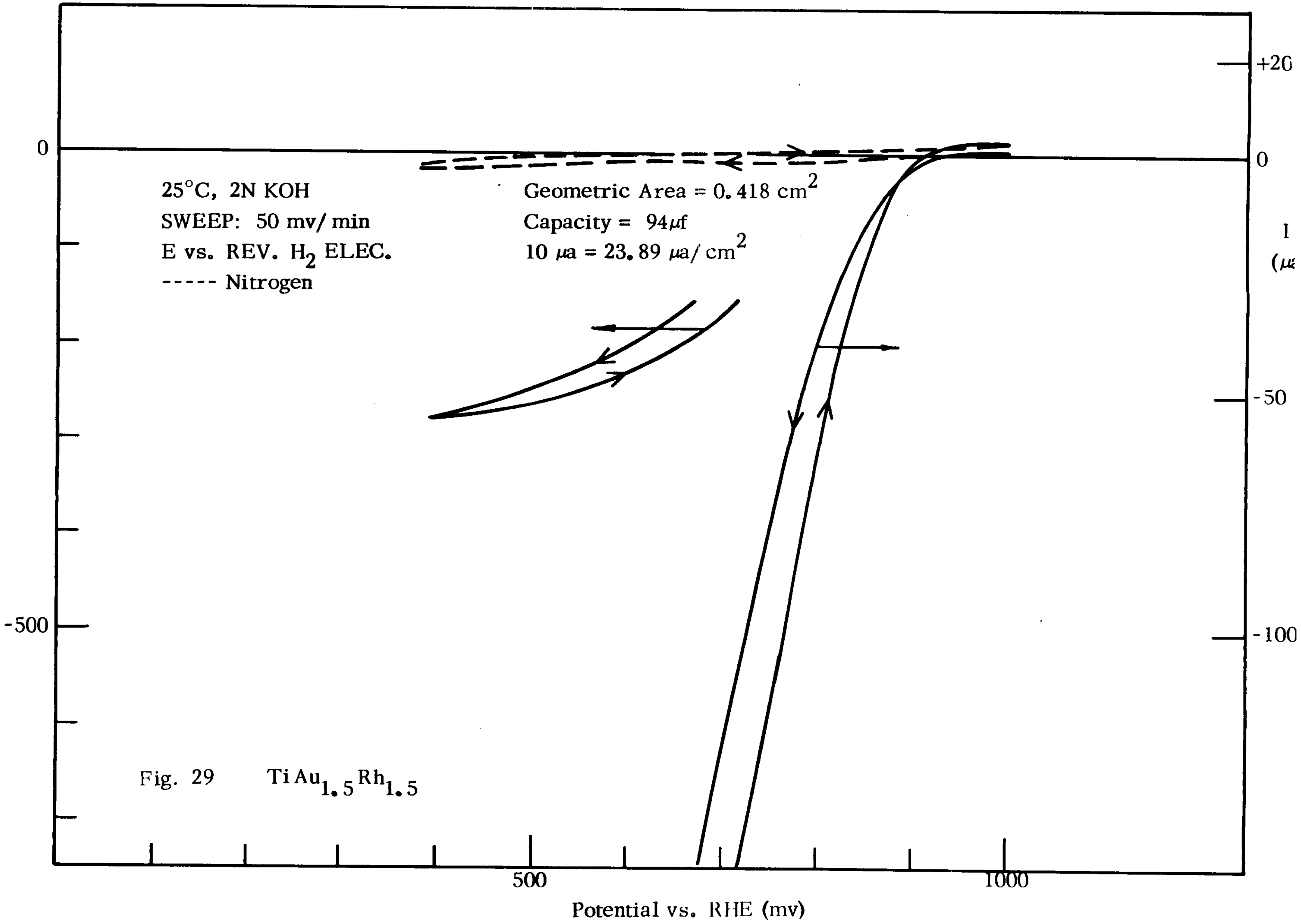

Fig. 29 Ti $Au_{1.5}Rh_{1.5}$

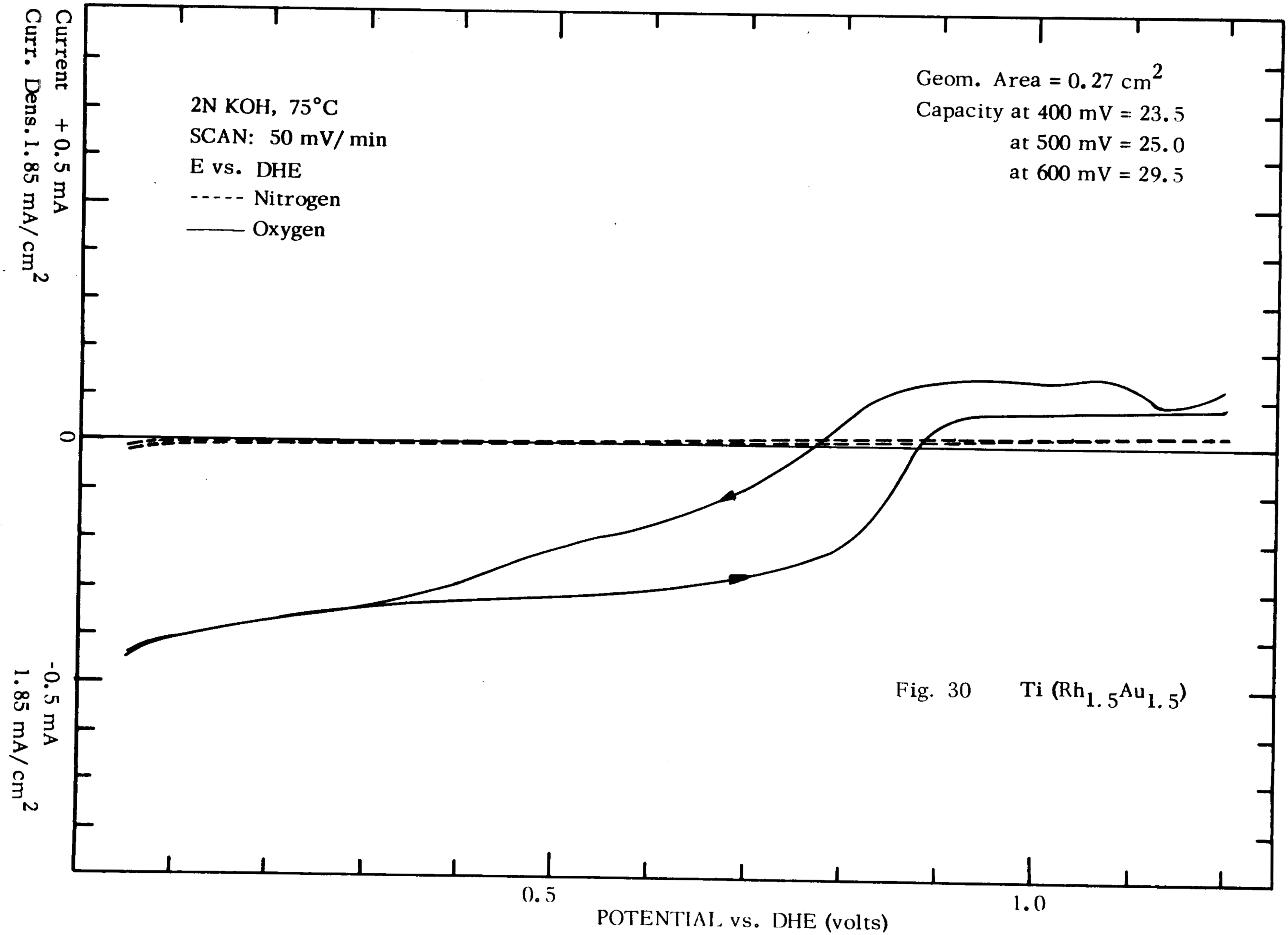

Fig. 30 Ti ($Rh_{1.5}Au_{1.5}$)

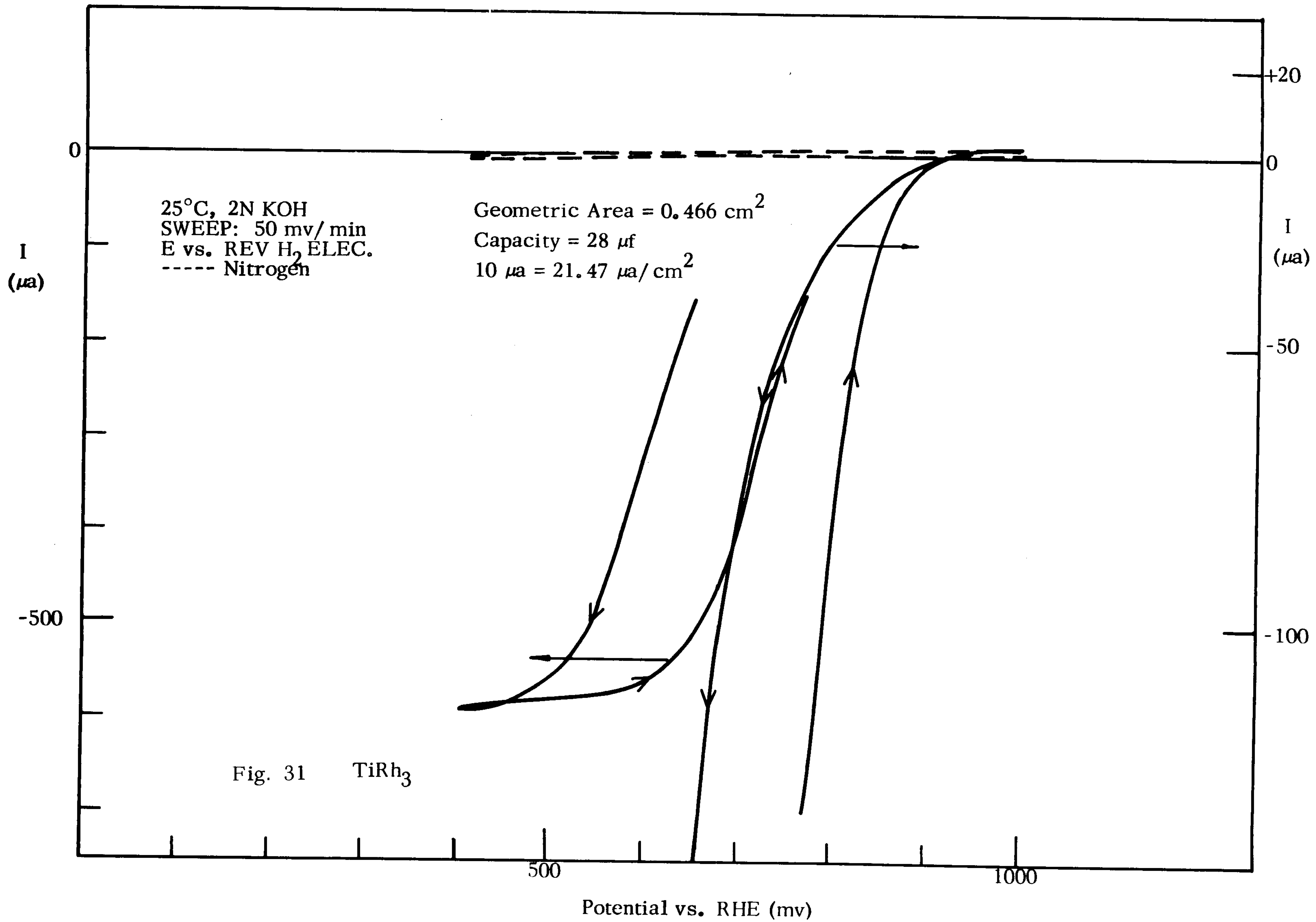

25°C, 2N KOH
SWEEP: 50 mv/min
E vs. REV H_2 ELEC.
----- Nitrogen
Geometric Area = 0.466 cm^2
Capacity = 28 μf
10 μa = 21.47 $\mu a/cm^2$
I (μa)
0
-500
+20
-50
-100
500
1000
Potential vs. RHE (mv)

Fig. 31 $TiRh_3$

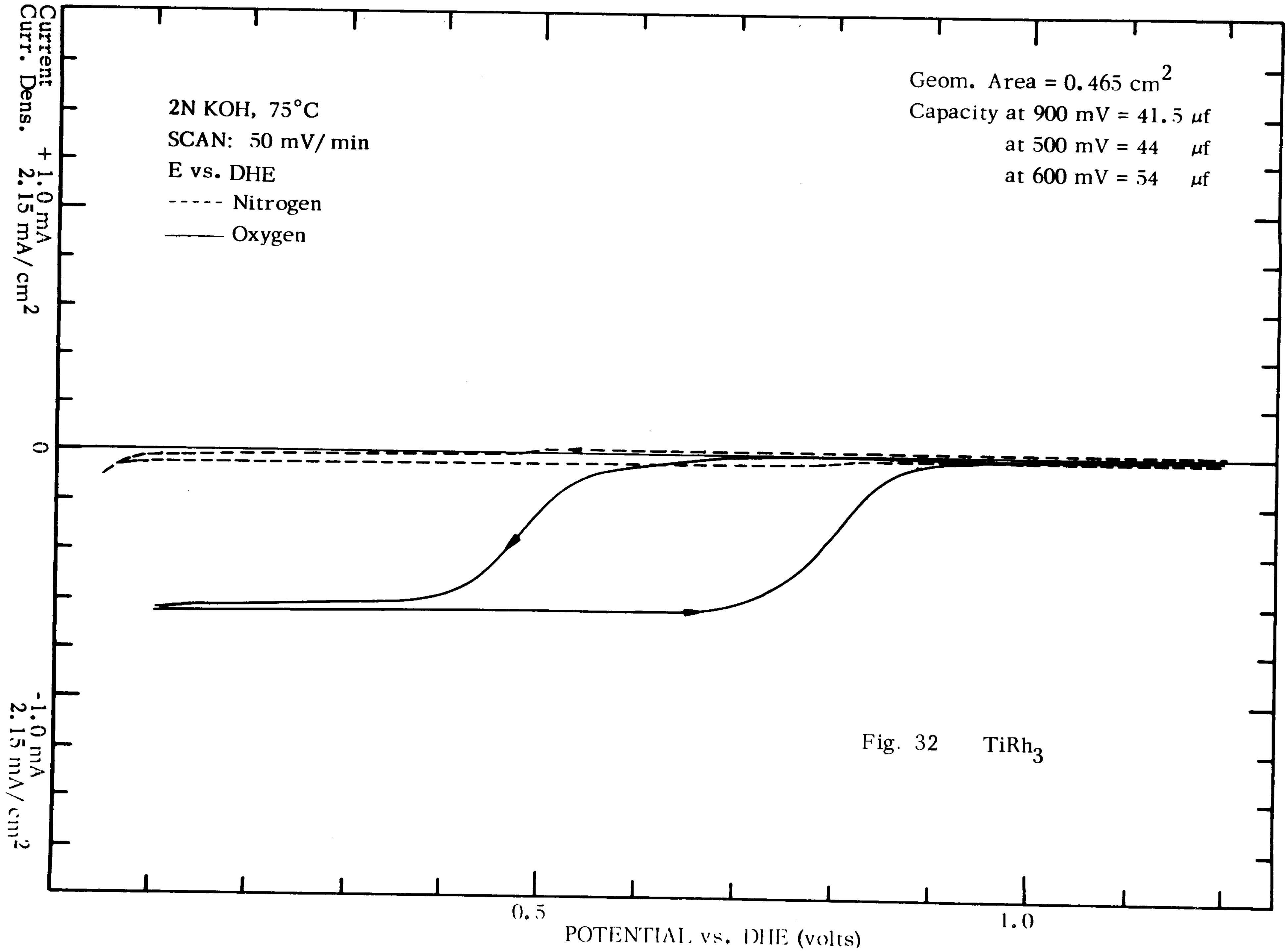
Current + 1.0 mA
Curr. Dens. 2.15 mA/cm2
0
-1.0 mA
2.15 mA/cm2
2N KOH, 75°C
SCAN: 50 mV/min
E vs. DHE
----- Nitrogen
—— Oxygen
Geom. Area = 0.465 cm2
Capacity at 900 mV = 41.5 μf
at 500 mV = 44 μf
at 600 mV = 54 μf
0.5
1.0
POTENTIAL vs. DHE (volts)

Fig. 32 $TiRh_3$

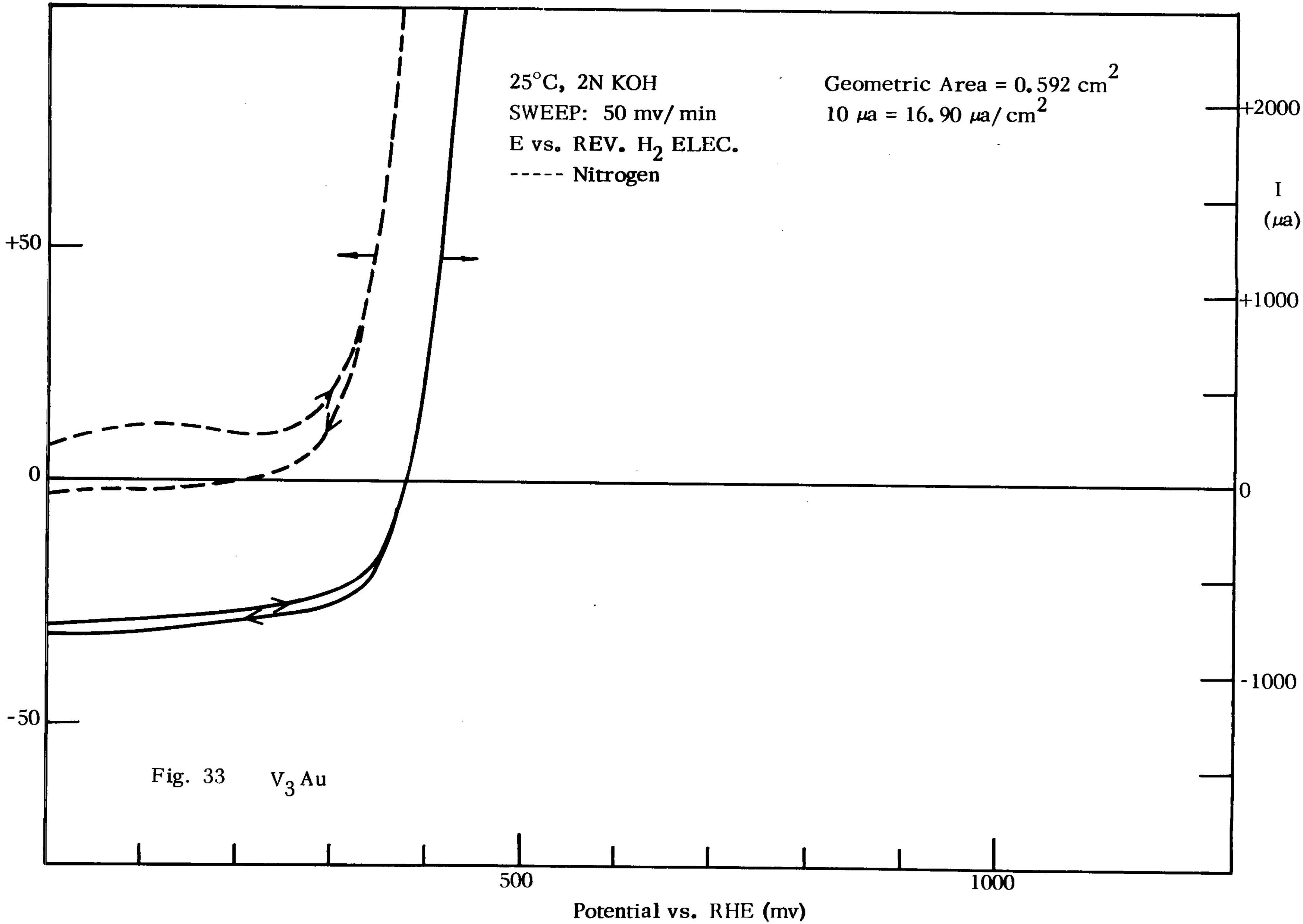

25°C, 2N KOH
SWEEP: 50 mv/ min
E vs. REV. H2 ELEC.
----- Nitrogen
Geometric Area = 0.592 cm2
10 µa = 16.90 µa/cm2
+50
0
-50
+2000
+1000
0
-1000
I
(µa)
500
1000
Potential vs. RHE (mv)

Fig. 33 V_3Au

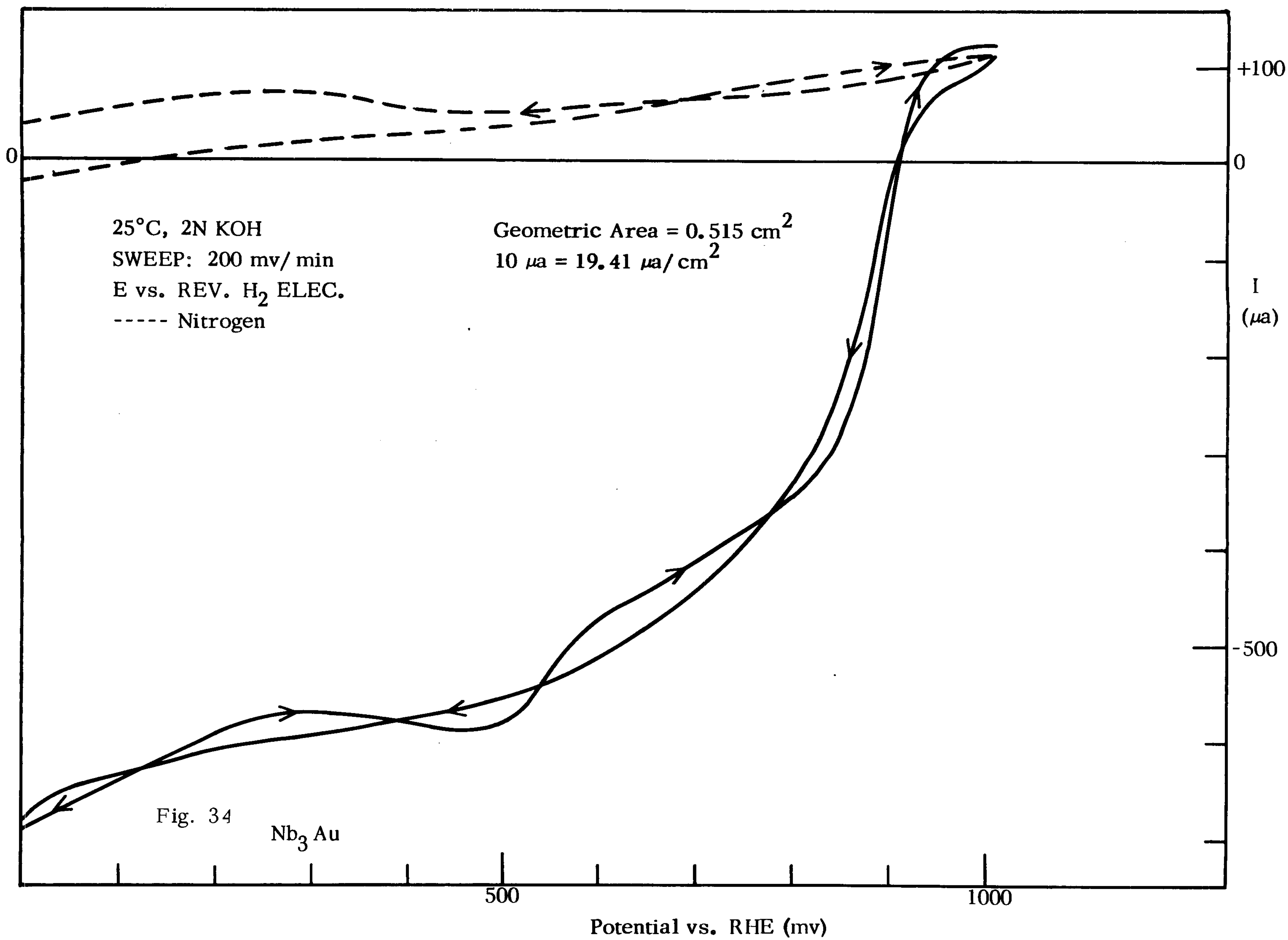
25°C, 2N KOH
SWEEP: 200 mv/min
E vs. REV. H_2 ELEC.
----- Nitrogen
Geometric Area = 0.515 cm^2
10 μa = 19.41 $\mu a/cm^2$
Fig. 34
Nb_3Au
0
+100
0
I (μa)
-500
500
1000
Potential vs. RHE (mv)

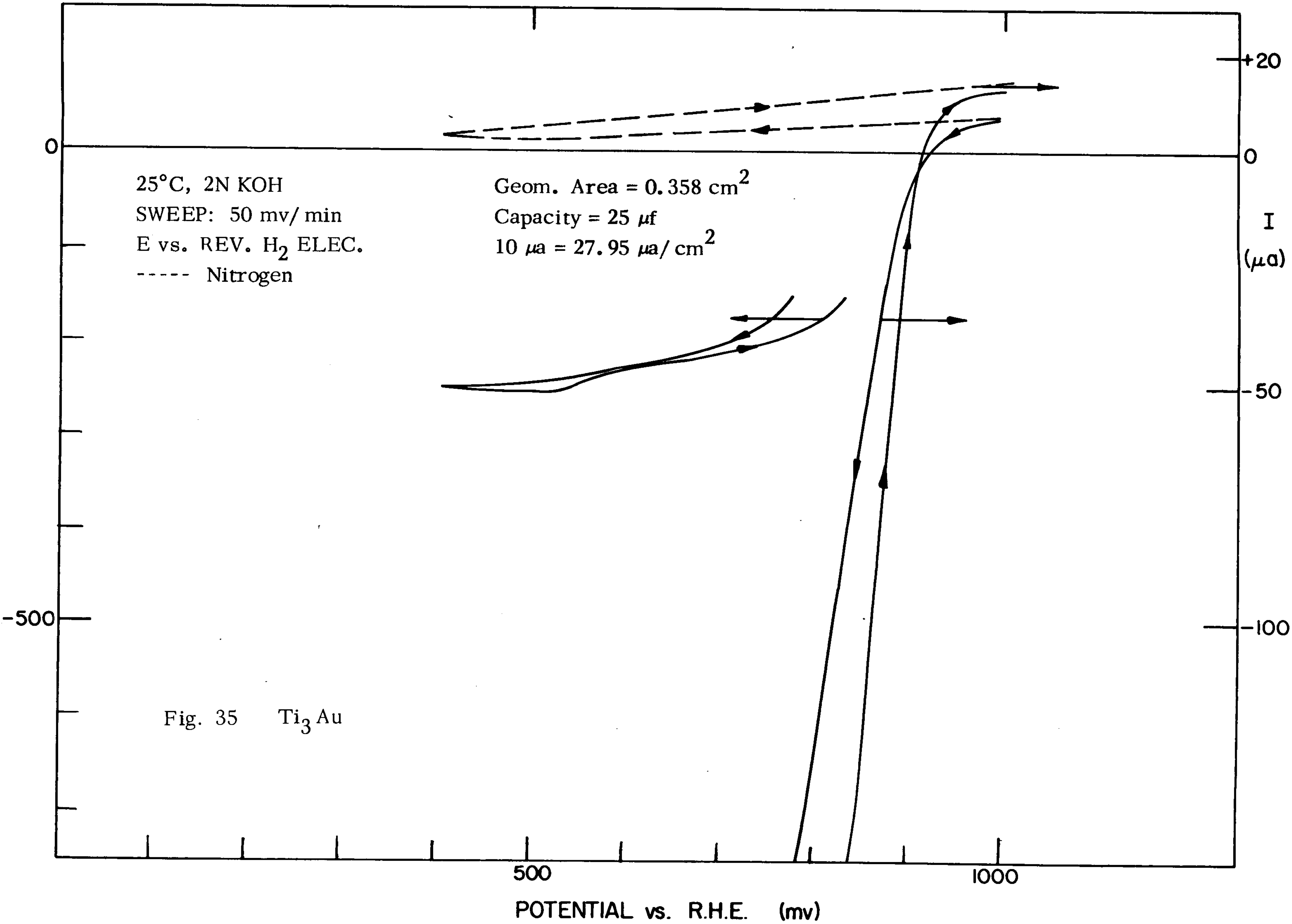

0
-500
+20
0
I
(μa)
-50
-100
500
1000
POTENTIAL vs. R.H.E. (mv)
25°C, 2N KOH
SWEEP: 50 mv/ min
E vs. REV. H_2 ELEC.
----- Nitrogen
Geom. Area = 0.358 cm^2
Capacity = 25 μf
10 μa = 27.95 μa/ cm^2

Fig. 35 Ti_3Au

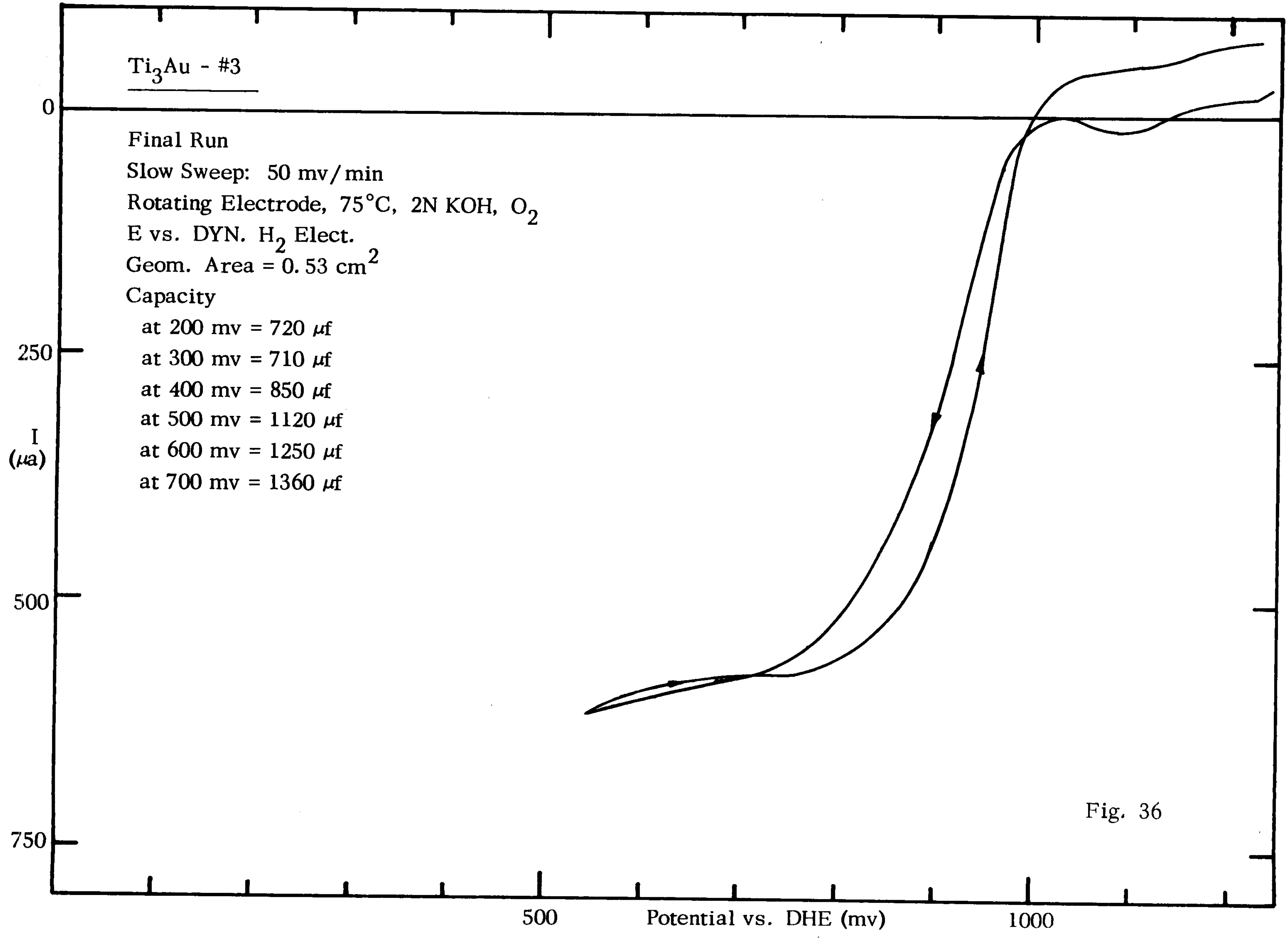
Ti_3Au - #3
Final Run
Slow Sweep: 50 mv/min
Rotating Electrode, 75°C, 2N KOH, O_2
E vs. DYN. H_2 Elect.
Geom. Area = 0.53 cm^2
Capacity
at 200 mv = 720 μf
at 300 mv = 710 μf
at 400 mv = 850 μf
at 500 mv = 1120 μf
at 600 mv = 1250 μf
at 700 mv = 1360 μf
0
250
500
750
I
(μa)
500
1000
Potential vs. DHE (mv)

Fig. 36